# Predicting fillability of viscoelastic product in Tetra Recart

Nawapan Boonchum and Roxanne Mae Targa

DIVISION OF PRODUCT DEVELOPMENT | DEPARTMENT OF DESIGN SCIENCES
FACULTY OF ENGINEERING LTH | LUND UNIVERSITY
2020

MASTER THESIS


This Master's thesis has been done within the Erasmus Mundus Joint Master Degree FIPDes, Food Innovation and Product Design.

Funded by the Erasmus+ Programme of the European Union

# Predicting fillability of viscoelastic product in Tetra Recart

## A case study with Tetra Pak

Nawapan Boonchum and Roxanne Mae Targa


LUND
UNIVERSITY

# Predicting fillability of viscoelastic product in Tetra Recart

A case study with Tetra Pak



*Published by*
Division of Packaging Logistics
Department of Design Sciences
Faculty of Engineering LTH, Lund University
P.O. Box 118, SE-221 00 Lund, Sweden

Subject: Food Packaging Design (MTTM01)
Division: Packaging Logistics
Supervisor:
Björn Bergenståhl, Prof., Dep. of Food Technology, LTH
Kristina Helstad, PhD, Tetra Pak® Packaging Solutions AB
Examiner:
Jenny Schelin, Division of Applied Microbiology, LTH

This Master´s thesis has been done within the Erasmus Mundus Joint Master Degree FIPDes, Food Innovation and Product Design.

www.fipdes.eu

# Abstract

It is of interest to design a methodology in predicting the fillability of non-Newtonian viscoelastic product such as meat batter by analyzing its rheological properties, reducing the need to perform pilot plant scale tests.

Meat batter with different added water produced in laboratory and pilot plant were analyzed to represent meat batters with different rheological characteristics and filling behaviour. The analysis of the rheological properties of the samples were performed in duplicates using rotational rheometer.

The rheological tests done include flow curve determination, build-up test, break down test, and amplitude sweep test. The results showed that the meat batter had shear thinning time-dependent property (thixotropy) and could be described by Power Law at shear rate range 1-200$s^{-1}$ which was applicable to the filling machine.

The calculated K value, apparent viscosity, and calculated Pressure drop derived from the model showed decreasing trend as the % water increased, which could provide information on the limit of the machine. On the other hand, the trend of n value which ranged from 0.10-0.15 was not dependent on the % added water. The samples with lower added water was found to have higher thixotropy and elastic property compared to those of more added water, which influenced its fillability.

The samples were tested in the filling machine to study the pressure profile curves. Samples which were able to be filled showed a steady state region and followed a viscous fluid behaviour. The prediction model was found to have a good estimation of the experimental pressure drop value for higher water added meat batter.

In conclusion, the calculated K value and amplitude sweep test can be used to predict the meat batter's fillability in the filling machine with a standard tank. For products which exceeded the limit, the filling machine with pressurized tank can be recommended.

**Keywords:** Meat batter, Filling machine, Rheology, Pressure drop, Non-Newtonian fluid

# Executive summary


**Introduction**

Increase in the trend of green consumerism has been observed as more consumers are becoming more concerned with the environmental impact of the products that they are purchasing. Thus, food manufacturers, specifically for canned products, are making the shift from metal packaging to a more sustainable material such as Tetra Recart®. The latter has been proven to have less environmental impact as compared to metal cans but still having the same properties needed to provide safe food products.

The Tetra Pak R2 Machine with the piston filler has been used to fill different types of food product for the Tetra Recart package®. The focus of the study is meat batter as it could represent viscoelastic products. To predict the fillability of the meat batter in TPR2 machine with standard product tank and when to recommend Pressurized product tank for products that exceeded the limit of the former, the study aims to achieve the following objectives.

**Objectives**

1.) To understand the rheological characteristics of meat batter with different formulations
2.) To investigate the product's rheological properties which can be correlated to its fillability in the TPR2 machine with standard product tank
3.) To understand the pressure drop in the filling pipe
4.) To correlate the meat batter's rheological properties and their corresponding pressure profile

## Hypothesis

The assumption is that the rheological parameters of the meat batter can be used to correlate with the pressure drop during the filling process. The specific hypothesis of the study includes:

1.) The use of rheometer can produce reproducible results to quantify and make a rheological model for the meat batter
2.) The rheological model established can be used to predict the pressure profile of the batter inside the filling machine
3.) The rheological characteristics of the different meat batter can predict the fillability of the product in the machine

## Materials and Methodology

The materials used for this study were pork belly class 3 (HKScan), pork shoulder class 2 (Martin&Servera), modified starch, salt, and water. The meat was cured, grinded, and mixed with other ingredients using different equipment for laboratory and pilot plant scale. The resulting products were meat batter samples with varying percentage of added water which had different rheological properties and fillability. These were analyzed in duplicates using rotational rheometer with the serrated cup and four-blade vane attachment.

The flow curves of the meat batter were analyzed, and a Non-Newtonian fluid flow model could be fitted. Also, the corresponding rheological parameters, and the thixotropy property were studied. Build-up and breakdown tests were performed to study the thixotropy property of the meat batter. Amplitude sweep test was also performed to analyze the viscoelastic property of the meat batter.

The K and n values were derived from the flow curves which were used to estimate the apparent viscosity. The estimated pressure drop was also calculated in order to compare with the experimental pressure drop.

The different meat batter samples were tested in the TPR2 machine with standard tank to gather data on the pressure profile and pressure drop curves. The experimental pressure drop values were then compared to the calculated pressure drop.

## Conclusions

The conclusions obtained from this study were:

1. The rheological characteristics of the meat batter could be studied using the vane geometry in the rotational rheometer which showed that the meat batter could be described by the Power Law Model. The rheological measurements provide K and n values of which the former decreased as the % added water was increased, while the latter was not significantly affected. Shear thinning behaviour was observed among all the samples. The calculated apparent viscosity and pressure drop estimated from the rheological measurements showed decreasing trend as the % added water was increased.

   The calculated K value and amplitude sweep test can be used to predict the meat batter's fillability in the filling machine with a standard tank and when to recommend the filling machine with pressurized tank.

   The values obtained from products produced in laboratory and pilot plant scale were not significantly different from each other.

2. The analysis of the flow curve could be used to study the thixotropy property of the meat batter which showed decreasing trend with the additional water. The filling duration is shorter than the time needed for the meat batter with lower %added water to build-up. The amplitude sweep test showed that the sample with lower water had more elastic property.

3. The pressure measurements during the filling in the machine showed the difference in the typical pressure profile curves for products with different fillability. The meat batters which were able to be filled in the TPR2 machine with standard product tank were 20% and 30% added water meat batter that followed the viscous fluid behavior. This showed the limit of the machine without pressurized product tank as no less than 20% added water. However, samples of 15% and 10% added water meat batter were not able to be filled exhibited more elastic property during the filling process.

4. The Rabinowitz-Mooney derived from the Power Law model used to predict the pressure drop of the meat batter samples was only applicable to 30% AWMB.

5. The fillability of the meat batter was significantly affected by its elastic property. The calculated pressure inside the piston for lower added water samples was found to be at the pressure in which water molecules could boil at 10°C which could create steam inside the piston. In addition, the

mixture of meat batter and air in the pipe might have affected the filling behavior of the samples.

**Recommendations**

The following are recommendations based on the study:

1. Meat batter products can be further investigated in terms of viscoelastic properties and adhesiveness/stickiness by Texture Profile Analysis. This is to further understand its behaviour and to study the possibilities to correlate to its behavior during filling.

2. The fat, protein and quantitative analysis of the meat particle size can be done to determine the effect of the meat composition and microstructure on its rheological properties. The effect of varying the fat content of the meat batter can also be studied and be correlated to its fillability in the machine, to know the applicability of the prediction model in different conditions.

3. More parameter of machine response could be studied to understand how the machine works and responds to the product. This may include the motor response, synchronization to the piston movement, and the pressure measurement in the piston.

4. Study of other fluid flow models including the elastic properties could be done to determine the best fit prediction model for the meat batter with lower added water.

5. To provide a substitute for meat batter in the machine test, further study in the proxy product could be performed such as build-up, breakdown and amplitude sweep in order to compare to the rheological properties of meat batter. Machine test of the proxy product could be made in order to gather pressure data measurements and to increase the understanding of machine fillability in a systematic way.

# Acknowledgments

We wish to express our sincere appreciation to the people whose support was a milestone in the accomplishment of this work. Firstly, our supervisor Professor Björn Bergenståhl, who dedicated his time to supervise and guide us throughout this study. The invaluable advises and analytical information that he gave helped us to go on with the experiments and analysis. Without his persistent help, the objectives of this work could not be fulfilled.

Secondly, we wish to show our gratitude to our supervisor from Tetra Pak, Kristina Helstad, for being patient with us and for providing support and assistance in organizing meetings and experiments with the Pilot plant machine. We also wish to thank co-supervisors from Tetra Pak, Fredrik Innings and Dragana Arlov who patiently gave us precious opinion on our work. We could not achieve the goals without their help.

We would also like to express our sincerest gratitude to other experts at Tetra Pak namely Klas Haglund, Peter Brunkestam, Peter Larsson, Mattias Rådström, Fredrik Nilsson, Anders Borgkvis, Göran Pantza, Björn Loodber, Björn Lindberg, Sten Sjostrom, Martin Nilsson, and Jannika Timander for helping us in conducting the experiments. Our sincere thanks also to the staff at Department of Food Technology, Engineering and Nutrition at LTH who were always willing to help us during the experiment.

Also, we would like to thank Erik Anderson and Jenny Schelin for their help as Program Coordinator and examiner. Lastly, we wish to acknowledge the encouragement from our family, FIPDes friends and friends at Lund University who supported and were with us along this journey. ขอบคุณค่ะ and maraming salamat po!

Lund, June 2020

Nawapan Boonchum and Roxanne Mae Targa

# Table of contents

# List of acronyms and abbreviations

| | |
|---|---|
| AWMB | Added water to meat batter |
| hPa | hectopascal |
| K value | Consistency index |
| n value | Flow behaviour index |
| PL | Power Law |
| $\Delta P$ | Pressure drop |
| $\dot{\gamma}$ | Shear rate |
| $\tau$ | Shear stress |
| TPR2 Machine | Tetra Pak® R2 Machine |

# List of Figures

# List of Tables

# List of Equations

# 1 Introduction

*This section presents the background, scope, objectives, and limitations of the study.*

## 1.1 Background

Canned meat products are one of the processed foods that gained popularity due to convenience and long shelf-life. According to the U.S. Census data and Simmons National Consumer Survey (NHCS), 102.18 Million of Americans used canned meat in 2019 and this number is predicted to increase to 105.45 Million after four years. (Statista, 2020) However, along with the increase of demand for canned products, the trend toward 'green' consumerism is also in the rise. Farmer (2013) emphasized the impact of the packaging and its sustainability to the performance of the brand. Metal cans have more environmental impact compared to other packaging such as glass and carton mainly due to the production of the virgin material.

The typical packaging for this type of product is tin can as shown in Figure 1. They either come in cylinder or in square shape. They are all made of metal with coated layer for food safety and are resistant to high heat and high-pressure treatment.


**Figure 1 The American luncheon meat brand 'SPAM' product by Hormel Foods. (Spam, 2019)**

One packaging that can replace the use of metal packaging for meat product is retortable carton packaging such as Tetra Recart® from Tetra Pak as seen in Figure 2. The packaging can undergo commercial sterilization process like canned food which provides the long shelf life for food product under ambient temperature storage. The combination of Aluminum layer, polymers and paper board, provides protection for food, resistance to retorting process, and sealability. (Lotzke and Nyberg, 2018) The benefits of this package include being user-friendly, lightweight

and space efficient as it saves 30% space used compared to traditional can and glass jar. These advantages contribute to its lower environmental impact. (Tetra Pak, 2015) According to Tetra Pak (2020), a study conducted by Institut für Energie- und Umweltforschung Heidelberg (IFEU) in 2017 showed that the carbon emission over the lifetime of Tetra Recart® is 81% lower than that of steel cans and glass jars. Another study conducted by the Procarton (2014) reflected that over 40% of the consumers recognized the brand packed in carton which is significantly higher than other types of packaging.


**Figure 2 The material structures of a Tetra Recart package.**

One of the machines used to fill products for Tetra Recart® is called Tetra Pak® R2 (TPR2) machine as seen in Figure 3. The filling can be based on pocket filler, piston filler and liquid filler. Piston filler is based on volumetric filling by piston machine that moves to a specific distance to fill the desired volume of the product. (Tetra Recart Technical Training, 2014) It has the flexibility to fill cartons with liquid or semisolid product in different size carton packages volume. The machine consists of integrated forming, filling and sealing automation function. It can operate with the maximum capacity at 6000 packages per hour.

**Figure 3 The filling and packing machine Tetra Pak® R2 (Tetra Pak, 2015b)**

Thus, it is the interest of the study to understand how viscoelastic products behave during the filling process and to know the limit of the machine. This can be done by understanding the rheological properties of the products to be filled and to correlate it with the pressure profiles during its filling along the pipe of the machine. This study aims to predict the fillability of different products in the TPR2 Machine with standard tank and when to recommend Pressurized tank for products that exceeded the limit of the former, using the mentioned correlation.

## 1.2 Research Problem and Question

Understanding the properties of the product being filled is necessary to know the parameters that could relate to the fillability to the TPR2 Machine. This can also provide information on the limit of the machine. Thus, this can be considered as preliminary evaluation of the product's fillability at the laboratory scale. This will reduce the need to conduct Pilot Plant scale filling test for products that are deemed unfillable, thus avoiding product loss.

The focus of this study are meat batters which have complex microstructure resulting to its Non-Newtonian behavior. Different interactions such as protein-water, protein-protein, and protein-lipid interactions take place in this colloidal suspension. (Zayas, 2012) Thus, this study will aim to answer these following research questions:

1. How to determine product's rheological parameters that can be correlated to the experimental pressure profile of the meat product during the filling process?
2. Can the rheological properties measured in the laboratory be used to predict the pressure profile in the filling machine?
3. How to decide on which filling machine configuration to recommend for a specific food product?

## 1.3 Objective

The focus of the master thesis is to predict the fillability of the viscoelastic product in the TPR2 machine which can be obtained by the following aims:

1.) To understand the rheological characteristics of meat batter with different formulations
2.) To investigate the product's rheological properties which can be correlated to its fillability in the TPR2 machine with standard product tank
3.) To understand the pressure drop in the filling pipe

4.) To correlate the meat batter's rheological properties and their corresponding pressure profile

## 1.4 Hypothesis

The rheological properties of the meat batter can be used to predict its fillability to the TPR2 Machine which includes the following hypothesis:

1.) The use of rheometer can produce reproducible results to quantify and make a rheological model for the meat batter
2.) The rheological model established can be used to predict the pressure profile of the batter inside the filling machine
3.) The rheological characteristics of the different meat batter can predict the fillability of the product in the machine

## 1.5 Limitations

This master thesis aims to understand the correlation between the rheological properties of the meat batter and their corresponding pressure profile while it is being filled in the machine. However, the study has limitations in terms of the following:

1.) Only meat recipe will be studied
2.) The change in formulation will be limited to the amount of water in the meat batter
3.) One cam curve or filling setting will be used for the machine tests
4.) Tests were only performed in the TPR2 machine with standard tank but not in the TPR2 machine with pressurized tank.
5.) Only the section from the tank to piston filler of TPR2 machine will be analyzed in this study

# 2 Literature Review

*This section presents research to guide the reader on the different literature study about the different topics that cover the scope of the Master Thesis.*

## 2.1 Meat Products

The comminuted meat product (CMP) consists of a complex matrix where an amount of solubilized protein acts as emulsifier in the meat batter. There are protein-water, protein-protein, and protein-lipid interactions that take place in this colloidal suspension (Zayas, 2012).

### 2.1.1 **Meat Batter**

True emulsion is a system in which immiscible liquid is dispersed in another liquid. Rather than classified as meat emulsion, the term 'meat batter' was suggested to be used for CMP. It differs from the true emulsion due to the dispersion of fat particles in a matrix of solubilized protein and other non-meat ingredients (Lonergan, Topel, and Marple, 2019).

Lonergan et al, (2019) defined Bind as "the capacity to attract and retain water and encapsulate fat". Meat has binding ability naturally from the proteins of lean skeletal muscle tissues. Despite the same type of meat, in each part of meat tissue has different binding qualities which lead to various abilities to produce good quality meat batter. Red meat from cow, pig, sheep and calf are mainly used as raw material in meat products as they have high lean-to-fat ratio which contribute to greater water binding capacity compared to poultry and other groups of animal meat. The protein of lean skeletal muscle tissue plays the main role on properties of the meat batter during processing and finished product's quality (Lonergan et al., 2019). Also, Hermansson (1985) as cited by Smith (2003) said that the texture and cooking yield of product correspond to the characteristics of microstructure and rheology of gel network. Meat batter's viscoelastic behavior is influenced by the instinct factors such as, available proteins and their conformation, the intermolecular chemical forces, and the distribution and migration of water. The external factors like temperature and other ingredients present in the system also influenced the changes

in its structure which reflected to its rheological properties (Ahmed and Ramaswamy, 2007)

### 2.1.2 **Raw Materials**

#### *2.1.2.1 Meat Proteins*

Myofibrillar proteins are responsible for binding water and encapsulating fat such as actin, myosin and actomyosin. They are water insoluble proteins thus, addition of salt to the lean meat portion will solubilize myofibrillar protein. This will enable the meat to hold additional water and fat droplet to form gel when heated. Due to its properties, this became the focus for developing meat emulsion (Mandigo and Sulivan, 2014).

Sarcoplasmic proteins are muscle pigment while myoglobin, a water-soluble protein is responsible for the color in meat. (Lonergan et al., 2019; Mandigo and Sulivan, 2014) Even though they have less binding capacity compared to myofibrillar proteins, these two are the main important proteins for meat batter (Zayas, 2012).

Stromal proteins or collagen is a connective tissue protein which has low binding capacity. It is located in many parts of animals including skin, ligament, tendons, cartilage and bone (Keeton et al, 2014). This protein can limit the stability of emulsion-type meat product production if it is present in high amounts in the raw material used in meat batter. (Lonergan et al., 2019)

#### *2.1.2.2 Meat Fat*

The content of fat in the product is one of the major ingredients which affect the texture, juiciness, taste, flavor and the final price. The characteristics of fat are also directly related to the emulsion stability. Many studies found that temperature influences the behavior of meat batter as it reflects on viscosity of batter that decreases when the temperature increases beyond the fat melting point. The consequence includes fat separation from other phases due to the density difference and its sensitivity to coalesce during the processing. Therefore, the recommended temperature at the endpoint of chopping of different types of meat are set as the general rule for manufacturing. The endpoint temperature should be below 18 °C for beef fat, 12 °C for pork fat, and 8 °C for poultry fat. (Mandigo and Sulivan, 2014)

#### *2.1.2.3 Non-meat Ingredients*

Varieties of non-meat ingredients are added by manufacturer for many reasons to improve the functional properties of products during processing, for organoleptic properties, to reduce cooking loss, to prolong shelf life of the products and to reduce the raw material cost. (Lonergan et al., 2019) Non-meat ingredients that are directly

related to enhance flavor are seasoning and spices. Different manufacturers use wide range of these ingredients, but there are essential ingredients that are commonly found in meat batter type products. These are salt, water and meat extenders or meat binders.

Salt is an essential non-meat ingredient added to the meat batter. (Honikel, 2010) It plays several roles in the product which mainly to facilitate the solubilization of myofibrillar protein. Due to its ionic property, it also increases ionic strength and the water holding capacity of the meat batter. Moreover, it reduces the water activity and enhances the flavor of the finished product. The general salt content in most sausages is 1.5-2.5% (Lonergan et al, 2019). While other products like Hot dog and Bologna usually have 2-3% of salt (Lawrence and Mancini, 2004)

Water is added for the processing and consumer satisfaction. In processing, water serves as medium for water soluble ingredients, for dissolving and dispersing curing ingredients and controlling the temperature. Water also affects the color, appearance and palatability (tenderness, juiciness and flavor). It is bound and entrapped within the sausage structure leading to the high-quality sausage products. The regulation limits the water content in fresh sausages and luncheon meat at 3% and the maximum allowable fat content is 30% in emulsion products. (Lonergan et al, 2019)

In order to get desired functionalities of the food product, starches are usually introduced to the food matrix. Aside from source of carbohydrate, starch could act as thickener, stabilizer, texturizer, binder, sweetener and processing aid. The comminuted meat products usually undergo extreme processes like high shear mixing and high thermal treatment. Therefore, modified starches are suitable to use as they can tolerant wide range of processing parameters, such as acidity, thermal conditions and mechanical shear while remaining its stability. They are multi-functional and cost-efficient food additives (Luallen, 2018). The additional of modified starch in meat batter significantly improve the binding capacity and emulsion stability which resulted in reduction of the fat separation (Aktas and Genccelep, 2006). For the final product, reduction of cooking loss was improved with the addition of starch (Li and Yeh, 2003).

### 2.1.3 **Meat Batter Processing**

Zayas (2012) stated several factors that affect the properties of meat batter which are temperature, salt concentration, size of muscular and connective tissue particles, size of fat droplets, pH, added proteins, shear force, autolytic state of the meat, handling of meat and so on.

The meat products that are prepared by finely comminuting the raw material to achieve raw high viscous batter then go through thermal treatment as shown in Figure 4. They are classified as ‘cold emulsion’ or raw-cooked products. (Honikel, 2010)

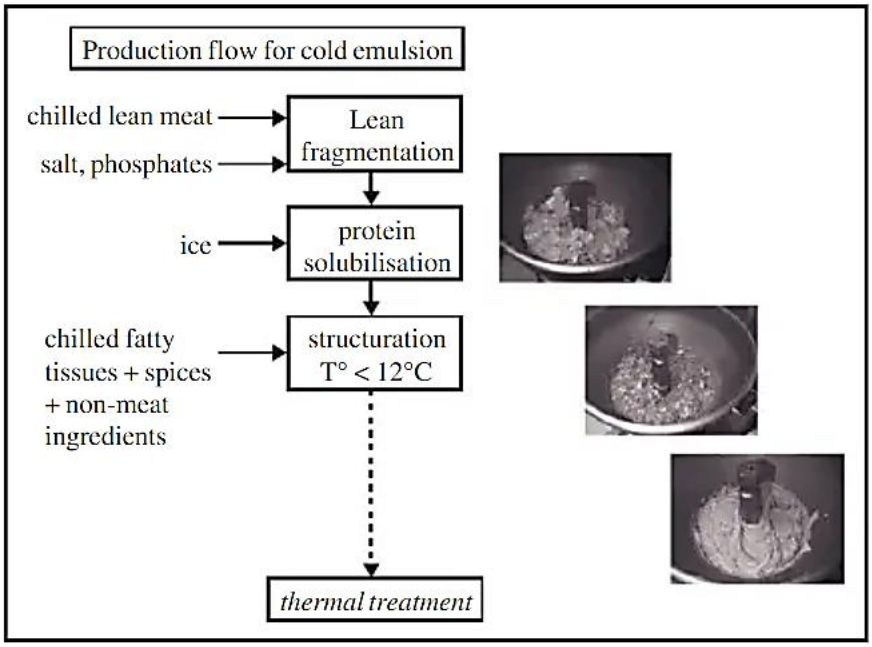


**Figure 4 The diagram of cold emulsion process. (Allais, 2010)**

Curing the meat is done during the manufacture of meat products with the addition of Sodium chloride (Salt) with or without nitrite and/or potassium nitrate. (Honikel, 2010) The function of salt is to partially solubilize myofibrillar proteins and to lower water activity. Polyphosphate, on the other hand, dissociates myosin which results to the lowering of the viscosity of raw meat emulsion. (Hui, 2012)

Meat undergoes the process of comminution which aims to reduce the particle size of the meat with the use of either grinder, bowl chopper, or flaker. The grinder includes the grinding plate and a knife in which the meat is pressed against resulting to the cutting of the meat. The hole size of the grinding plate determines the size of the meat product. (Hui, 2012) On the other hand, the bowl chopper includes a revolving bowl and a rotating metal knife that cuts and mix the meat as it revolves. The last machine is flaker which can be used for frozen meat by pressing the knife blades unto the meat to cut the meat. (Hui, 2012) They are needed for the mechanical processing as they provide the required shear rate during grinding and blending of meat batter. The solubilized proteins as emulsifiers would coat the surface of fat particles, muscle particles, connective tissue and other non-meat particles in the system and bind them together. (Mandigo and Sulivan, 2014; Honikel, 2010 and Zayas, 2012) The equipment with vacuum condition for mixing could facilitate removing of air in batter and increasing of product density. During chopping and mixing, the temperature of batter needs close monitoring, because the equipment can increase the batter temperature. As Pearson and Gillett (1999) as cited by

Lawrence and Mancini (2004) investigated that the meat batter will be destabilized and loss its functionalities if the temperature exceeds the melting temperature of fat.

## 2.2 Rheology

Rheology is based on the concept in Greek called "panta rhei" which means everything flows. It is defined as the science of understanding the deformation and flow of matter. (Steffe, 1996) The concept can be applied to all types of materials, gases, liquid and solid. It studies how matter respond to different stresses and strain. Its application in the food industry includes process engineering calculations for designing food manufacturing equipment. (Steffe, 1996)

In food science, rheology is used for explaining product's consistency and flow behaviour of different products. As stated by Mathisson (2015), in order to study flow behaviour and structure of food product, shearing must be applied. The flow can be induced by introducing shear through flow between parallel planes, rotational flow between stationary cylinder and rotating cylinder which are coaxial, telescopic flow in capillaries and pipes, and torsional flow between parallel plates.

The rheology property of a material is studied using the correlation between stress and strain. Zhong and Daubert (2013) defined the former as the force with magnitude and direction that is applied to a specific area. Normal stress is when the force is applied perpendicular to the surface generating change in length, ΔL extension while shear stress is when it is applied parallel to the surface resulting to angular deformation $\gamma$ as seen in Figure 5 below.

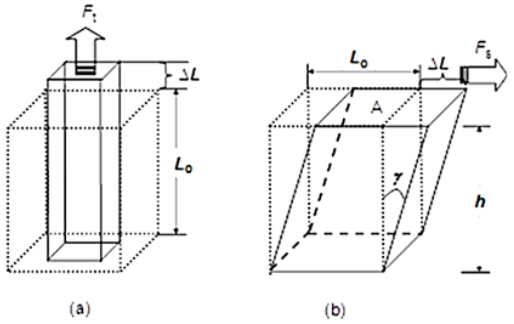


**Figure 5 Difference between a tensile deformation. (Zhong and Daubert, 2013)**

Shear strain, γ, is defined as the result of applied shear stress producing difference in the velocity. On the other hand, shear stress, $\tau$ (Pa), is "stress component applied tangentially" and is equal to the force vector divided by area of application. (Rao, 2014) Viscosity, η (Pa-s), is the fluid's internal friction and its tendency to resist

flow. Strain reflects the relative displacement or deformation in terms of magnitude and directional. The relationship between stress and strain or strain rate in different shear is used to classify the rheological properties and types of flow. (Dogan and Kokini, 2006)

### 2.2.1 **Newtonian Fluids**

Newtonian fluids are those that exhibit a proportional relationship between $\tau$ and $\gamma$, with the dynamic viscosity, $\eta$ as the constant of proportionality, in constant temperature and pressure. (Deshpande, Krishnan, and Kumar, 2010) Substances with low molecular weight such as organic or inorganic liquids, inorganic salts, molten metals, salts, and gases are examples of these. Chhabra and Richardson (1999) defined the equation for incompressible Newtonian fluid in laminar flow that can explain this relationship as:

$$\tau = \eta\dot{\gamma} \tag{1}$$

The flow curve or "rheogram" is the plot of the shear stress against shear rate. A Newtonian fluid has straight line passing through the origin with a slope, $\eta$ as seen in Figure 6b.

A system that is exhibiting yield stress which is defined as the start of the flow of a material at specific value of stress, $\tau_0$ is considered as the Bingham plastic fluid. (Rao, 2014) The relationship is:

$$\tau - \tau_0 = \eta'\dot{\gamma} \tag{2}$$

### 2.2.2 **Non-Newtonian Fluids**

Substances that do not follow the Newtonian flow characteristics are called Non-Newtonian fluids. Irgens (2014) defined the viscosity function $\eta(\dot{\gamma})$ as apparent viscosity which is dependent on the shear rate applied to the fluid. The flow curves of different fluids show distinguish behaviour between the relation of shear rate to viscosity and shear stress are illustrated in Figure 6.

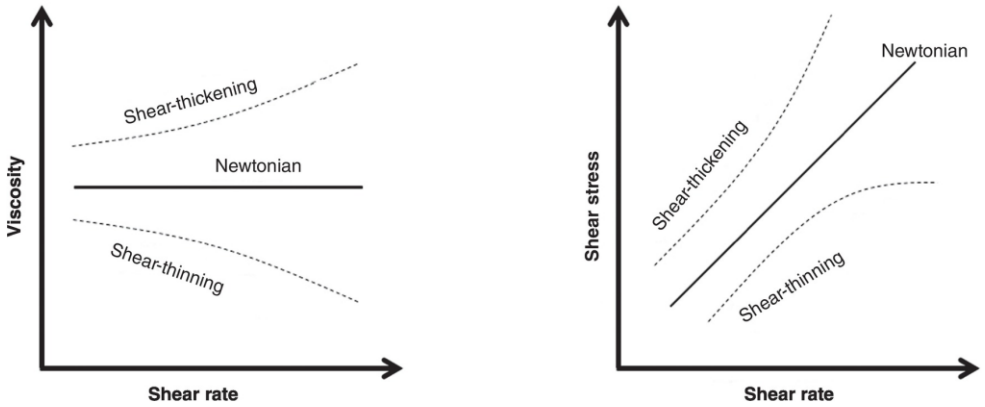


**Figure 6 Flow curves of Newtonian and Non-Newtonian Fluid (a) Viscosity against Shear rate (b) Shear Stress against shear rate (Hozefa Ebrahim, Sunita Balla, James Rudge, 2019)**

Different time-independent flow behaviours are exhibited by food systems as described by Rao (2014) below. The model that describes shear-thinning and shear thickening fluids if the data are plotted on double logarithmic coordinates is the Power Law model:

$$\tau = K\dot{\gamma}^n \tag{3}$$

in which *K* is the consistency coefficient or consistency index (Pa) and *n* is the flow index (dimensionless). For Newtonian fluid, K is equal to the viscosity and n =1 while the fluid is shear thinning if n<1 and shear thickening if n>1.

For power law, once the log τ are plotted against log γ, a linear regression could be used to predict the values of K and n. Using the equation below, the straight-line intercept is computed as K and the slope is n. (Rao, 2014)

$$\log \tau = \log K + n \log \dot{\gamma} \tag{4}$$

On the other hand, another rheological fluid model that can explain the properties of food product is the Herschel Bulkley Model. It is based on the concept of having a yield stress that needs to be overcome for the product to flow. A fluid that follows Herschel Bulkley model is called yield pseudoplastic material. (Rao, 2014) The model expresses with following equation:

$$\tau - \tau_0 = k\dot{\gamma}^n \tag{5}$$

The power law model is mostly being used because it is the simplest model to describe non-Newtonian fluid. However, it has the disadvantage of not defining the low-shear and high-shear rate constant-viscosity of shear-thinning foods. (Rao, 2014)

*2.2.2.1 Shear Thinning Behavior*

Pseudoplastic or shear-thinning products' viscosity decreases as the shear rate increases. Most shear thinning fluids exhibit Newtonian behaviour with very low

and very high shear rates of which the apparent viscosity experienced by the fluid are called as zero shear viscosity, $\eta_0$ and infinite shear viscosity $\eta_\infty$, respectively. (Chhabra and Richardson, 2008) This in turn means that the apparent viscosity of the fluid with increasing shear rate of a specific fluid ranges from $\eta_0$ to $\eta_\infty$. Figure 7 illustrates the typical shear thinning behaviour of fluid plotted between viscosity and shear rate.

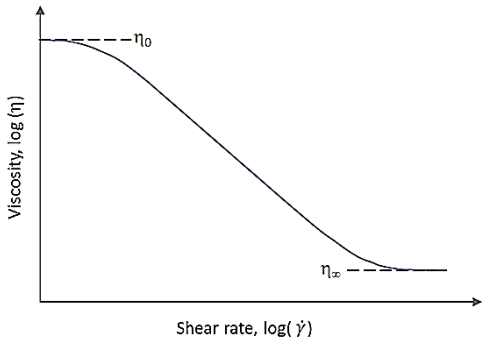


**Figure 7 The typical behavior of fluid with shear thinning property (Crow, 2015)**

Shear thinning behavior could be expressed with the Power Law equation of Oswald and de Waele, which combined with apparent viscosity definition. This type of fluid shows declining slop (n<1) with the increasing of shear rate that contributes to small apparent viscosities at high shear rate. (Zhong and Daubert, 2013) The apparent viscosity of Power law fluid could define as:

$$\eta = K\dot{\gamma}^{n-1} \tag{6}$$

Some materials, on the other hand, exhibit an increase in the viscosity as the shear rate increases and are called shear thickening or dilatant fluid. This behaviour could also describe by the apparent viscosity equation above, with the n-value greater than one. (Crow, 2015) When the fluid is at rest, there is minimum amount of free spaces as the liquid fills the gap. However, increase in the applied shear rate forces the solid particles to expand or dilate resulting to not enough fluid to fill the gap. This, in turn, increases the solid to solid contact, thus increasing the friction and shear stress, consequently the viscosity of the fluid. (Chhabra and Richardson, 2008)

*2.2.2.2 Viscoelastic Property*

Zhong and Daubert (2013) explained ideal solid product as elastic or follows a spring analog which deforms proportionally with the force. Mechanical analogs can be used to explain the viscous and elastic property of a product as seen in Figure 8. The ideal solid product stores this energy and springs back as the force is removed. On the other hand, for viscous or ideal liquid, the applied force is converted into another form of energy as the piston of the dashpot after the force has been exerted. Most of the materials have both elastic and viscous properties which can be explained by the Maxwell model of viscoelasticity. In this model, if force is exerted

upon a material, the energy is being stored in the spring while being dissipated by the dashpot. (Lin, 2011)

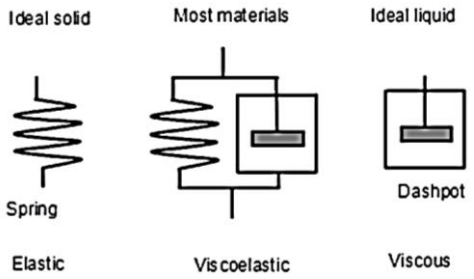


**Figure 8. Mechanical Analogs describing different materials. (Zhong and Daubert, 2013)**

The proportionality of deformation caused by stress can be explained by Hooke's Law in the Equation (7). (Zhong and Daubert, 2013)

$$\tau = G\gamma \tag{7}$$

in which τ is shear stress, γ is shear strain, and G is elastic shear modulus. On the other hand, for liquid products, Newton's Law of viscosity can explain the relationship between shear stress and shear strain rate by viscosity, η with the following equation.

$$\tau = \eta\dot{\gamma} \tag{8}$$

*2.2.2.3 Amplitude Sweep*

Huang, Li, and Summer (2012) described amplitude sweep test as an oscillatory movement of the geometry at a specific frequency and variable amplitude which ranges from small deformation until the maximum shear deformation. The shear modulus can be classified as storage modulus or elastic part of deformation, G' which can be calculated by the expression:

$$G' = \frac{\tau_A}{\tau_A} cos\delta \tag{9}$$

and loss modulus or viscous part of deformation,

$$G^{"} = \frac{\tau_A}{\tau_A} sin\delta \tag{10}$$

The subscript A pertains to the amplitude of deflection while δ is the phase shift angle that quantifies the reaction of the material to the shear stress in terms of viscous part. At δ=0˚ (tan δ=0), the material is behaving in ideal elastic and is deforming ideal viscous at δ=90˚ (tan δ= ∞). (Huang et al, 2012) The cross over point at δ=45˚ in which the G' is equal to G" shows the flow stress of critical stress, σ*. Beyond this shear, the viscous part of deformation is dominant which will result to the flow of the product. (Anton Paar, 2020)

### 2.2.3 **Time-Dependent Behavior**

The behaviour of a fluid not only depend on the shear rate but on the time that it has been sheared. Depending on the type of fluid, the amount of linkages that are being destroyed when the fluid is being sheared affects the rate of change in the viscosity. (Chhabra and Richardson, 2008) On the other hand, the increase in the breaking down of structure also increases the rate of which these linkages can reform. Thus, a balance of breaking down and building-up of the structure can result to dynamic equilibrium. (Chhabra and Richardson, 2008)

#### *2.2.3.1 Thixotropy*

Thixotropic materials are those which experience a reduction of apparent viscosity with the time of shearing. It forms a hysteresis loop for a flow curve which is exhibited when the material is sheared from zero to a maximum value in a constant rate of increase and then decreased to same rate to zero value (see Figure 9). The hysteresis could be described as the area between sweep up and down curves where the rate of breakdown during up curve was greater than the build-up rate. (Koehler, et al, 2014)

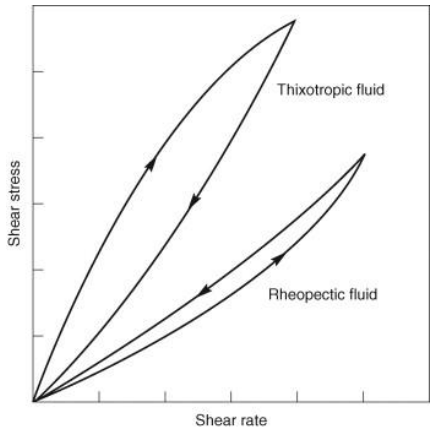


**Figure 9 Thixotropy Behavior (Chhabra and Richardson, 1999)**

The area, height, and shape of the loop are dependent on the length and rate of increase/decrease of shear and on the historical kinematic of the sample. (Chhabra and Richardson, 2008) The product can also build-up the structure once the shearing is stopped and the product is allowed to rest for a period of time. Those materials which exhibit an increase in the viscosity as the shear rate increases are called rheopectic or negative thixotropic fluid. They also formed hysteresis loop but the resulting shape is inverted. (Chhabra and Richardson, 2008) This means that the material structure is building up as it is being sheared while breaking down when the material is at rest.

*2.2.3.2 Break down and Build-Up*

When the constant shear rate is applied to the material, the linkages that form the internal structure are broken down as result in gradually decreasing of apparent viscosity. This phase is reversible and is determined as break down. The rate of apparent viscosity drops to zero as the consequence over time. Contrarywise, the rate of linkage re-forming is also raising as the structures are broken down, thus the dynamic equilibrium reaches the balance between break down and build-up rates. Therefore, for the material exhibiting thixotropic behavior, the broken down of structure is reversible as the shearing is removed and resting time is applied to let the structure build-up whereby the viscosity could recover to the original value. (Chhabra and Richardson, 2008) The break down and build-up of structure are reflected with decreasing and increasing of apparent viscosity and are illustrated in Fig. 10 associated with the thixotropy.

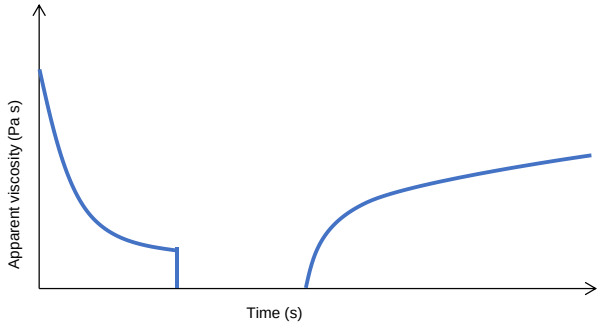


**Figure 10 The apparent viscosity during break down and build up**

The breakdown test is performed by exposing the sample to constant shear rate at specific time to analyze the viscosity plateau of the sample. (Muhammad, 2020) The initial apparent viscosity ($\eta_i$) and the final sampling point $(\eta_f)$ were compared and reported in percentage of difference. Noted that the initial apparent viscosity is taken when the target shear rate was reached, therefore the first 10 sampling points are ineligible. This could compare the rate of break down across samples and the effect of different shear rate applied to samples. The percentage of break down in the considered period can be calculated by Equation (11).

$$\%\ Break\ down = \frac{\eta_i - \eta_f}{\eta_i} \times 100 \quad (11)$$

The build-up test is performed by applying high pre-shearing followed by time to rest ($\Delta t$). After that, the sample is sheared at lower shear rate to measure the build-up of the structure. The shear rate applied to the sample during build up test is presented in Figure 11. The structural parameter, λ is computed by the following Equation (12) as described by Wei, et al (2016) The structural parameter value is between 0-1 where 0 is interpreted as the structure is completely destroyed and 1 means that the structure is completely recovered. (Wei et al., 2016)

$$\lambda(t) = \frac{\eta(t)-\eta_\infty}{\eta_0-\eta_\infty} \quad (12)$$

The η(t) is the viscosity of the sample after Δt at which the desired shear rate is reached and $\eta_\infty$ in the viscosity value when it reached steady state. The initial viscosity, $\eta_0$ is derived from a control sample that has not been pre-sheared and is sheared by low shear rate with the same duration. This parameter, λ can be converted into percentage by 0% means no build up and 100% means totally recovered structure.

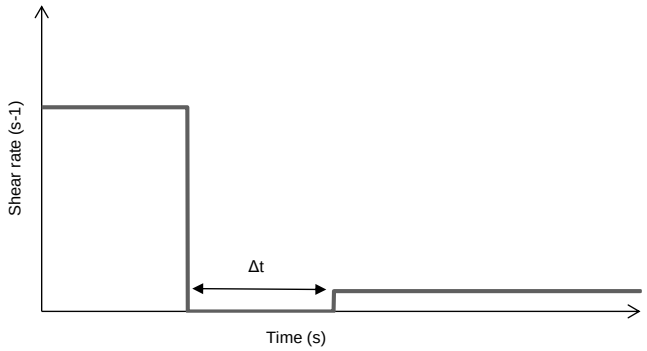


**Figure 11. The illustration of shear rate and resting period (Δt) applied to the sample for build-up test**

### 2.2.4 **Rotational Rheometer**

Rheology of food is studied using different laboratory equipment such as rotational and tube type rheometer. The particles will rearrange and deform due to the bonds in food structure are broken when shear is applied. Oscillating shear with low amplitude is applied to material thus the structure is not destroyed in oscillatory mode. Therefore, it is possible to study the elasticity of material. (Mathisson, 2015) The characteristics of majority of food materials have viscoelastic property. They behave both of elastic and viscous. This property is beneficial for predicting the processing and storage stability of the food products. (Dogan and Kokini, 2006) Rotational rheometers are sophisticated instruments for rheological analysis. They are operating with torsional vibration or oscillation. Therefore, they can be used in steady shear or in oscillatory mode. The purpose of measurement should be defined before performing to cover the representative range of shear rate and temperature during processing which is the focus of the application. The condition of temperature and timing are strongly related to the application, closer connection to the actual process will provide more applicable information. (Mathisson, 2015)

*2.2.4.1 Vane Geometry*

The vane of four to eight blades in cup geometry for rotational rheometer has being used to analyse product rheological properties (see Figure 12). A vane is composed of thin blades attached around a cylindrical shaft of small diameter. (Chhabra and Richardson, 2008) It has the advantages of being applicable to available rotational rheometer; is widely used for dispersions to prevent apparent slip; and has minimum effect to the microstructure of the sample as the attachment is inserted. This is relevant for thixotropic products as the recovery time may be too long. (Savarmand et al, 2007) This is also advantageous for material with mechanically weak structure such as gel and colloids. Some sample with thixotropic property could be very sensitive with the structure recovery. Therefore, using vane tool could be extensive with the complex type fluid. (AZO Materials, 2013)

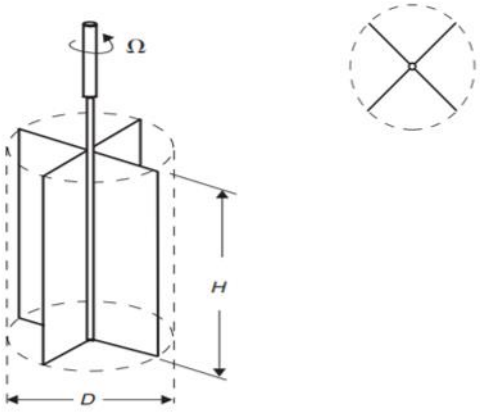


**Figure 12 Schematics of a vane used for measuring yield stress in viscoplastic systems (Chhabra and Richardson, 2008)**

# 2.3 Filling System

## 2.3.1 **Volumetric Filling System**

One of liquid filling techniques is volumetric filling. Figure 13 illustrates the basic principle of this technique. Knowlton and Pearce (2013) described the principle behind the volumetric filling system. The suction stroke begins when the piston is moving backward with clockwise rotation of cam. The empty cavity in cylinder with vacuum condition drives the flow of product from the hopper and determines the desired volume of the product as the displacement of piston is adjusted at the same time. When the position of piston is reached, the cam will start to move anti-clockwise to push out the measure product with return stroke through filling nozzle. The advantage of the method is the high productivity with accurate volume

delivered. It is very flexible technique and suitable for high viscous products. (Knowlton and Pearce, 2013)

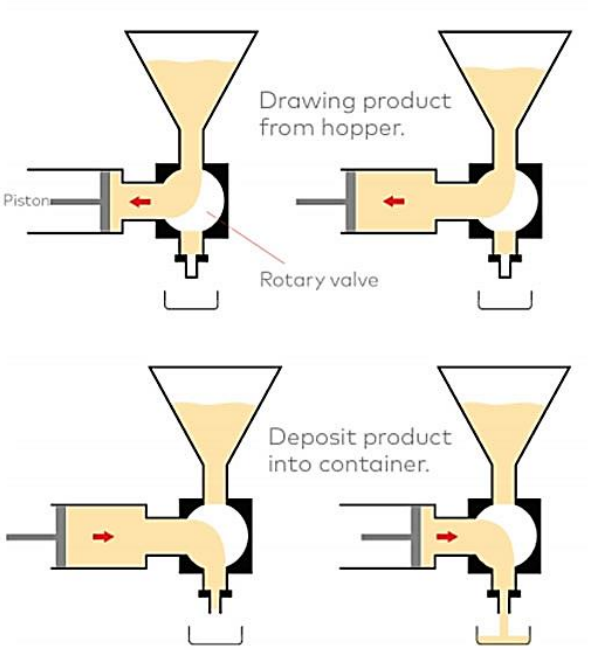


**Figure 13 The piston filler principle for filling application (Npack, 2020)**

*2.3.1.1 Simplified Diagram of TPR2 Machine*

Figure 14 shows the simplified version of the TPR2 machine which emphasizes the section from the product tank (2) to the filling head (7). The product tank on top of the machine is equipped with agitator (1). It helps maintain even temperature of product inside tank, facilitates the flow by pushing the product down the pipe and/or prevents sedimentation during filling by mixing. There are two pipes from the product tank and each is connected to piston filler (5) through rotational front valve (4). The front valve controls the inlet and outlet steam of the product to the dosage cylinder of piston filler. It will be in down position to open and let the product fill the dosing head during suction stroke. The volumetric filling principle is applied to this machine system. The amount of fluid product will be measured in the piston as the distance changes with the constant diameter of dosage cylinder. The movement of piston can be controlled and adjusted to suit with the food product properties. After the product has been filled in the cylinder, the valve will close and it will be

in up position to open to the outlet pipe. The flatted carton packages with multi-layers carton blanks will be loaded manually to the machine. (Tetra Recart Technical Training, 2014)

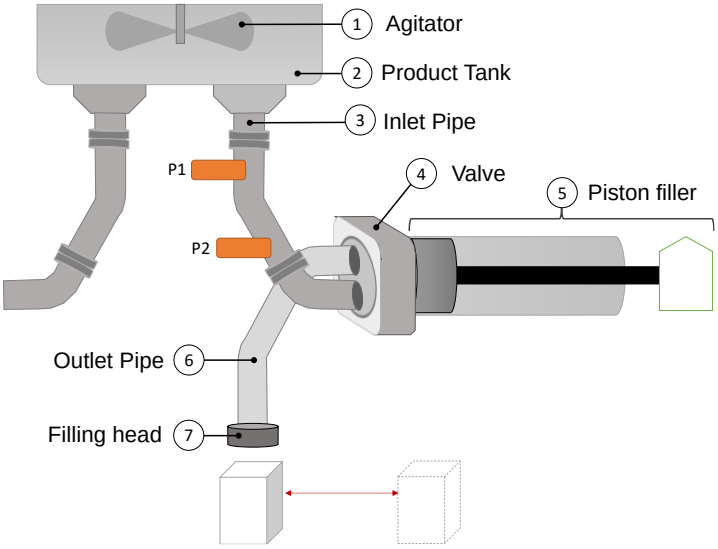


**Figure 14 The simplified diagram of filling system of Tetra Pak R2 filling Machine with the additional installation of pressure meters.**

Package blanks will be formed and ready to be filled with the product. The formed packages will be transported via conveyor belt under the filling head. Then the measured product will be pushed into the package through the filling head and the package will be sealed with pressure and heat. Filled packages will go through the next process of retorting in which the food will be treated with high heat and pressure during the commercial sterilization. (Tetra Pak, 2015b)

# 2.4 Correlation of Pressure Drop and Rheological Properties

## 2.4.1 **Newtonian Fluid Flow**

### *2.4.1.1 Fluid at Rest Pressure drop*

When there is no flow in the pipe, the pressure of stand still fluid at difference vertical elevation is distinct. Hydrostatic distribution is the pressure distribution that indicated the depth of incompressible fluid is increasing as the depth is increased. (Munson, Young, Okiishi and Huebsch, 2009) This relationship could be expressed in the following Equation (13).

$$P_1 - P_2 = \rho g h \quad (13)$$

Where h is the height of fluid between two points called the pressure head, $\rho$ is the density of fluid, g is the gravity acceleration, and $P_1$-$P_2$ is the difference of pressure. Therefore, the pressure of incompressible fluid at rest depends on the distance of fluid from the referenced level. The size or shape of fluid container does not affect the static pressure. (Munson et al, 2009)

*2.4.1.2 Fluid during flow*

The types of flow could be determined by dimensionless number given by Osborne Reynolds. This number is called Reynolds number (Re) which represents the ratio between inertial and viscous force. It is directly related to the transport properties of fluid. (Rapp, 2017) Reynolds number reflects the different flow characteristics. When Re is low, the viscous forces are dominant therefore, the flow is laminar. In contrast, the flow with higher Re is turbulent and the inertial force is dominating. (PhillipEllenberger, 2014). The general range of Re for laminar flow is below 2000, the transition flow is between 2000 and 4000 and the turbulent flow is above 4000. (LaNasa and Upp, 2014) The simplest form of Reynolds number for the flow in pipe can be expressed in Equation (14).

$$Re = \frac{\rho v D}{\mu} \quad (14)$$

Where ρ is the density of the fluid, v is the velocity of fluid, D is the internal diameter of the passageway and μ is the dynamic viscosity. Note that the unit of all parameter need to be the same basic since the Re result is dimensionless.

To evaluate the pressure loss in difference type of flow in circular pipe, the Darcy-Weisbach Head loss ($h_f$) equation can be used as the following Equation (15).

$$h_f = f \frac{L}{D} \frac{v^2}{2g} \quad (15)$$

where $f$ is the Darcy-Weisbach friction factor and it is dimensionless. It is a good flow resistance coefficient which represents both laminar and turbulent flow. The value of $f$ will be calculated or read differently according to the type of flow determined by Reynolds numbers. The $f$ for laminar flow (Re<2000) in circular pipe is defined as:

$$f = \frac{64\mu}{\rho v D} = \frac{64}{Re} \quad (16)$$

And for the turbulent flow case, $f$ could be estimated by basing from the Moody diagram shown in Fig.15. The use of Moody diagram comes with assumption of flow that it is fully developed, steady and incompressible flow. The diagram is based

on the boundary roughness ($\frac{\varepsilon}{D}$), the Reynolds number (Re) and the pipe radius (r).

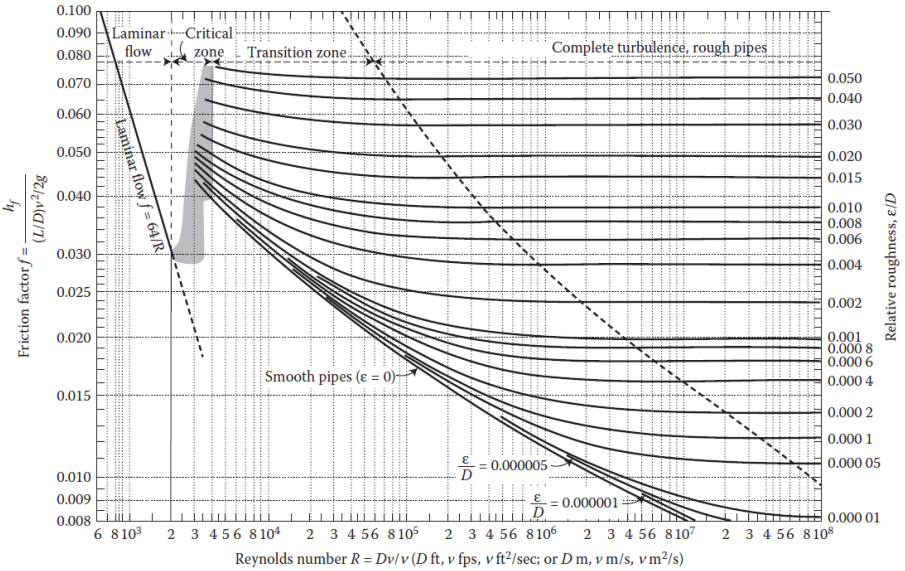


**Figure 15. Moody Diagram (Moody 1944 as cited by Shalaby, 2018)**

The relative pipe roughness ($\frac{\varepsilon}{D}$) can be calculated by the quotient of the absolute pipe roughness and the diameter of pipe. The $f$ value could then be obtained from the diagram using the $Re$ and ($\frac{\varepsilon}{D}$) values. The pressure drop ($\Delta P$) in turbulent flow could be expressed by substituting the relationship with shear stress in pipe flow into the Darcy-Weisbach head loss equation as the following Equation (17). (Shalaby, 2018)

$$\Delta P = f \frac{L}{D} \frac{v^2}{2} \rho \tag{17}$$

### 2.4.2 **Non-Newtonian Fluid Flow:Power Law Model**

The wall shear rate for Power Law fluid can be derived from the Hagen poiseuille equation with Rabinowitsch-Mooney correction factor and is given by the equation (Smith, 2003):

$$\dot{\gamma}_w = \left(\frac{3n+1}{4n}\right)\left(\frac{8v}{d}\right) \tag{18}$$

In which $v$ is the velocity of the product and d is the diameter of the pipe. Since the Rabinowitsch-Mooney correction factor for shear-thinning fluids (n<1) is always greater than 1, Newtonian fluids will always have greater wall shear rate than that of shear-thinning fluids.

Assuming that the pipe is circular, the velocity can be converted to flow rate by multiplying it with the area of the pipe. Thus, the wall shear rate can be written as:

$$\dot{\gamma}_w = \left(\frac{3n+1}{4n}\right)\left(\frac{4\mathrm{Q}}{\pi r^3}\right) \tag{19}$$

The wall shear stress, $\tau_w$ equation is given as

$$\tau_w = \frac{\Delta \mathrm{P}}{2}\frac{r}{\mathrm{L}} \tag{20}$$

Using the Power law model equation, the estimated pressure drop can be calculated using the following equation.

$$\frac{\Delta P \cdot r}{2 \cdot L} = K \cdot \left(\frac{3 \cdot n+1}{4n}\right)^n \left(\frac{4 \cdot Q}{\pi \cdot r^3}\right)^n \tag{21}$$

The stress-shear rate curves should reflect the application in the flow of the material inside the pipe. If the flow property data are gathered and are deemed reliable, the zero shear and the infinite shear flow curves are then used to design the flow system by setting boundaries. Chhabra and Richardson (2008) said that the maximum apparent viscosity (zero shear) and minimum apparent viscosity (infinite shear) can be used as the lower bound and upper bound limits for a flow rate with fixed pressure drop. On the other hand, the zero and infinite shear can be used to set the minimum and maximum pressure drop for a fixed flow rate system.

# 3 Methodology

*This section presents the materials, procedures, and calculations that will be used for the whole research.*

## 3.1 Materials

Different % of added water meat batter (AWMB) compositions were investigated as tabulated in Table 14 Appendix B. The different added water content was 10%, 15%, 20%, and 25% (w/w). These formulations were studied to understand the rheological characteristics and pressure profile of meat batter with different fillability and viscoelastic properties. These were comprised of pork belly class 3 (HKScan), pork shoulder class 2 (Martin&Servera), modified starch, salt, and water. The pork materials were delivered from the suppliers in Malmö, Sweden. The skin of the pork belly was removed, and the fat layer was maintained. The pork belly was cut up to 20mm thickness while the pork shoulder parts were already precut. The meat parts were stored in the chiller at 4-5°C before the preparation or in the freezer at –18 °C and were thawed 24hrs before curing.

## 3.2 Sample Preparation

### 3.2.1 **Laboratory Scale**

#### *3.2.1.1 Curing and Grinding*

The pork belly (approx. 20 mm) and pork shoulder (approx. 15mm) were mixed with salt as seen in Appendix B. The mixture was placed in a stainless-steel container, wrapped with Polyethylene stretch film and stored in the chiller at 4-5°C to cure for 12-15hrs. The cured meat was then grinded using Philips mincer (1800W, 2.3kg/min) up to 2mm final size as seen in Figure 16. The grinded meat was stored in the freezer (-18 °C) for at least one hour to reach the temperature no more than 2°C before mixing.

**Figure 16. Mincer for Laboratory scale Mixing**

The cured meat was mixed with modified starch and water (at least 10°C). The mixture at 500g batch was grinded using Robot Coupe R302 V.V. (see Figure 17) for 2 minutes at maximum speed with 30 seconds interval to scrap the sides of the mixer, until the desired final size was attained. The final mix was placed in a Ziplock bag and was kept at ambient temperature prior testing for rheological properties.


**Figure 17. Robot Coupe 302**

### 3.2.2 **Pilot Scale**

#### *3.2.2.1 Curing and Grinding*

The same procedure for meat preparation was used for the industrial scale. The mixture of meat and salt was placed in a rectangular Stainless-Steel container and was covered with Low Density Polyethylene plastic wrap. This was stored in the blast chiller at 4°C to cure for 12-15hrs. The cured meat was then grinded using Meat grinder LM-5/P (Koneteollisuus Oy, Finland) with the final blades up to 2mm final size (see Figure 18). The grinded meat was stored in the blast freezer (-18 °C) for at least one hour to reach the temperature no more than 2°C before mixing. Figures 46-49 in Appendix B show the images of cured and grinded meat.

**Figure 18. Meat grinder LM-5/P**

*3.2.2.2 Mixing*

The cured meat was mixed with modified starch and water (at least 10°C). The mixture was grinded for 5 minutes using Dadaux Titane 20 Bowl Cutter (Dadaux Technology, France) mixing at 10kg batch with the maximum speed (see Figure 19). The mixer was allowed to grind the meat while water was slowly added to the mixture until the desired size particle was obtained. The final temperature of the mix was controlled at 10-12 °C. The final mix was placed in a Stainless-steel container and was immediately brought to the Filling Machine for Testing. The final meat batter obtained after mixing in bowl cutter and ready for the next filling process showed in Figure 46 in Appendix B.


**Figure 19. Dadaux Titane 20 Bowl Cutter**

## 3.3 Sample Analysis

All tests performed were done in duplicate of which two samples from the same batch were measured consequently.

### 3.3.1 **Rheological Property Analysis**

The machine used for the analyzing the rheological properties of the meat batter was Malvern Kinexus Pro. Figure 21 shows the rheometer and the cup and vane geometry used. The sample volume used for the rheometer testing was fixed at 35g per load for the vane geometry. No calibration was performed for the machine and the gap height was set at 1.000 mm, with the default setting of maximum load and lowering rate of geometry. Detailed procedure for using the Rheometer and the rSpace software is in the Appendix C. Different geometries such as plate to plate, cup and bob, and cup and vane were used for preliminary tests and the vane and cup proved to be the most appropriate for the sample analysis as this reduced potential wall slip and unwanted destruction of the sample due to large particle size as discussed in Appendix D.

The timeline for testing laboratory scale meat batter (blue text) and the pilot plant scale (green text) is presented in Fig 20. The laboratory scale meat batter was immediately tested after the meat batter production. For the Pilot plant scale, there was a time gap of at least 240 mins between the production and testing in the rheometer. The meat batter was kept at 4 $^{o}$C before the rheological testing was performed and was stored at ambient temperature during testing.


**Figure 20 Timeline of Laboratory scale and Pilot Plant scale for rheological measurements**

### *3.3.1.1 Materials*

Temperature controlled Malvern Kinexus rheometer (Malvern Instruments limited Worcestershire UK) rSpace for Kinexus software (Figure 21)

Vane geometry, 4V213C0001 SS

Serrated cup geometry, 27.5 mm diameter, PC25G A0008 AL


**Figure 21 Rheometer (India Mart, 2020), Serrated Cup and Vane Geometry**

### *3.3.1.2 Stabilization time*

Stabilization time was determined based on Tetra Pak internal protocol. The sample was sheared at 200$s^{-1}$ for 5 minutes. The difference in the viscosity values at 10sec-interval was computed. The stabilization time was recorded when the % viscosity difference was less than 5% which meant that the equilibrium has been attained. This was done to ensure that the viscosity measurements were recorded when the system has reached equilibrium. Figure 22 shows the graph of viscosity values against time.

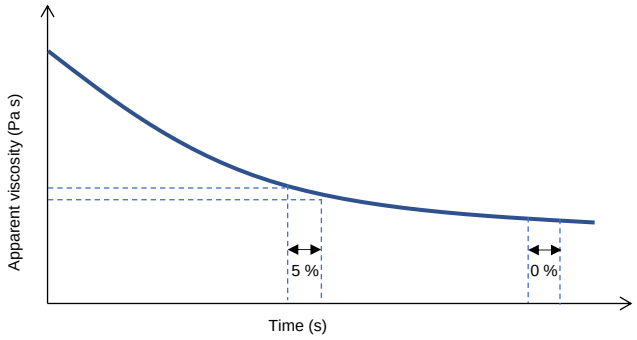


**Figure 22 The apparent viscosity plotted over time with the Tetra Pak protocol to determine the stabilization time**

The effect of pre-shearing was analyzed to confirm the need to preshear the samples. Different pre-shearing parameters with varying time and shear rate were employed for the analysis as seen in Table 1.

**Table 1 Pre-shearing variables**

| *Variables* | *Shear rate ($s^{-1}$)* | *Time (s)* |
|---|---|---|
| 1 | 100 | 120 |
| 2 | 10 | 90 |
| 3 | 1 | 30 |
| 4 | 0 | 0 |

Based on the preliminary experiments performed, the pre-shearing parameter of $10s^{-1}$ for 90sec was found to be sufficient for the sample as discussed in Appendix E.

*3.3.1.3 Determination of Rheological Parameters*

The sequence used for the final analysis of the meat samples had the following parameters:

1. Preshearing:$10s^{-1}$ for 90sec. This is proven to be enough for the sample to reduce the variability of the samples.
2. Samples per decade:2. Two sampling points were recorded per decade of shear rate.
3. Shear rate range: 0.1-$200s^{-1}$. The shear rate decided upon was based on the application to the industrial use which is during filling of the product. Inclusion of higher shear rate such as $200s^{-1}$ could provide wider range

4. Temperature:10°C. The lower temperature was selected to imitate the temperature of the meat while being filled in the machine.
5. Sweep: The sample was sheared with increasing shear rate range of 0.1, 0.3163, 1, 3.162, 10, 31.62, 100, and 200 $s^{-1}$(sweep up) and continued to decreasing shear rate range of 200, 63.25, 20, 6.325, 2, 0.6325, 0.2, and 0.1 $s^{-1}$ (sweep down)

The data gathered from the sequence are shear stress, shear rate, and viscosity. The shear stress values are plotted against the shear rate values in order to compute for the rheological parameters such as consistency index (K) and flow behavior index (n) using the Power Law model. The Ordinary Least Square (OLS) method was used to solve the rheological parameters by minimizing the sum of the squares of the residuals from the fitted and the experimental values. The linear curves were also analyzed in terms of logarithmic scale for both axes and the full range of shear rate for sweep up was selected for the OLS method.

*3.3.1.4 Thixotropy Properties*

Breakdown Test

The breakdown test was performed by exposing the sample to constant shear rate at specific time to analyze the viscosity plateau of the sample. Revisions were made to Muhammad (2020) break down test in which the shear rates were changed to lower values which were appropriate to the vane geometry and to the application during the filling. Table 2 below shows the different shear rates used with one sampling interval per second.

**Table 2 Constant Shear rates and Time of Measurements**

| ***Constant shear rate ($s^{-1}$)*** | ***Measurement Time (s)*** |
|---|---|
| 10 | 300 |
| 50 | 300 |
| 100 | 300 |

Build-Up Test

The build-up test was performed by applying high pre-shearing for 5mins at 10 $s^{-1}$. Then the sample was allowed to rest with different time ($\Delta t$) as tabulated in Table 3. After that, the sample were sheared at 1$s^{-1}$ for 15mins. Figure 23 shows the schematic representation of the shear rates for sample and control. Subsequently, the data were collected and were used to calculate for the structural parameter, $\lambda$ with the Equation (12). The calculated values were converted into percentage for comparison across meat batters.

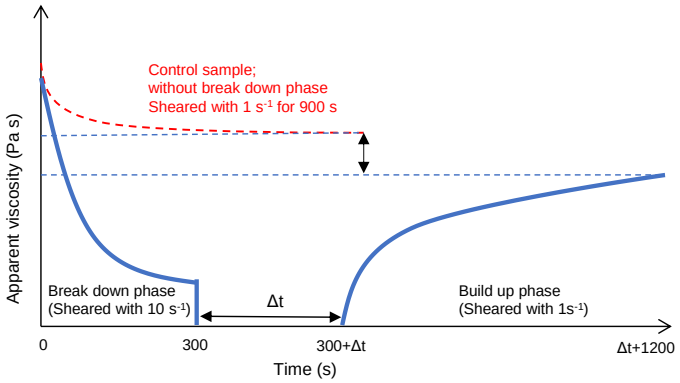


**Figure 23 Schematic of apparent viscosity meat batter during Build up test**

**Table 3 Shear rates and corresponding time for Build-up Test**

| ***Pre-shear Step (s-1)*** | ***Time interval (s)*** | ***Build-Up Shear rate (s-1)*** |
|---|---|---|
| 0 | 0 | 1 |
| 10 | 0 | 1 |
| 10 | 30 | 1 |
| 10 | 90 | 1 |
| 10 | 300 | 1 |

Hysteresis Loop Measurement

The sweep up and sweep down with range of selected shear rate obtained the flow curve. This hysteresis loop test evaluates the thixotropic property of sample. The shear stress response to the shear rate applied was observed during the sweep and compared the difference of initial shear stress and the shear stress at the final sampling point. This percentage of difference is then used for comparing the thixotropic between the sample. (Muhammad, 2020) The percentage difference of hysteresis loop is presented in Figure 24.

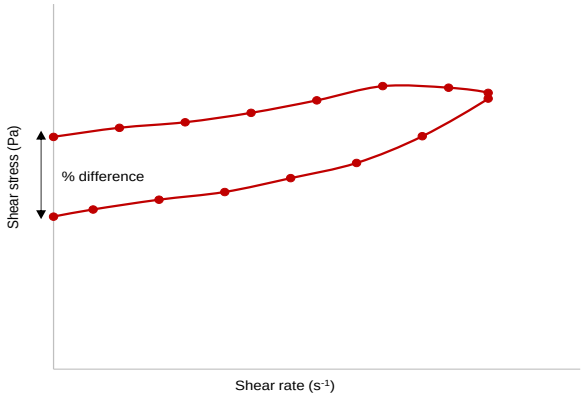


**Figure 24 Schematic of hysteresis loop**

*3.3.1.5 Viscoelastic Properties*

The amplitude sweep was performed on a rheometer with serrated cup and vane attachment of which the temperature is controlled at 10˚C. Approximately 30g of the sample was carefully loaded to the cup and was allowed to equilibrate for 5mins. It was done by subjecting the meat batter to shear rate range of 1 to 1000Pa at constant frequency of 1Hz. The storage or elastic modulus, G', loss or viscous modulus G", and phase angle, δ were plotted against shear stress range. The critical stress, σ* at which the δ is at 45° was determined.

## 3.3.2 **TPR2 Machine Setting and Calibration**

*3.3.2.1 Machine Setting*

The pressure meter sensors (PMP23, Serial Number R208110116B Endress Hauser) shown in Figure 25 were attached to the pipe located below the tank (P1) and before the piston (P2) with 175mm height difference between the two sensors as seen in Figure 14. The values obtained were corrected using the calibration factor as discussed in Appendix F. The cam curve used was for viscous product and the frequency of the agitator was set at 30Hz at clockwise direction of mixing. The capacity setting was set to 3000packages per hour (pph) which was half the capacity to allow enough time for the product to be cut and be filled to the packages.

**Figure 25. Pressure sensor**

The total cycle time is 2400ms in which 420ms was allotted for filling the product inside the piston and valve opening time took 40ms. The package used was TRC 390 Midi (maximum filling volume of 390mL) and the temperature setting was maintained at 10°C.

*3.3.2.2 Machine Calibration*

Before the testing of the meat product, water was allowed to run into the machine. Pressure measurements for both sensors were logged into the Pressure Logging Software. The data gathered for the water test including water temperature, level of water in the supply tank, height between two pressure meter and pressure measurement were used to calculate for the pressure drop during static condition for Newtonian behavior to compare with the calculation. This was performed to validate the conditions set in the experiment.

*3.3.2.3 Machine Testing*

The 50kg meat batter was transferred into the supply tank. The logging of the pressure started before the first stroke was done. The machine was allowed to run for few strokes to remove the water remained inside the pipe as the machine was not self-draining. Once it was ensured that all the water had been removed in the pipe, the machine was stopped for few seconds and was restarted again to fill the packages with meat batter. At least 50 packages were filled in order to attain sufficient amount of data for the pressure drop analysis. After the run, Cleaning-in-Place (CIP) was performed.

# 4 Results and Discussion

*This section provides the results of the research and the corresponding analysis to further obtain the objectives of the study.*

## 4.1 Meat Batter Rheological Properties

### 4.1.1 **Meat Batter Flow Curves**

The data of shear stress ($\tau$) versus shear rate ($\dot{\gamma}$) of duplicate samples were plotted in logarithmic scale. The upward sweep curves were fitted with Power Law (PL) model Equation (3) to obtain fitted line 1 and 2 for the experimental curve 1 and 2 accordingly as shown in Figures 26 and 27.

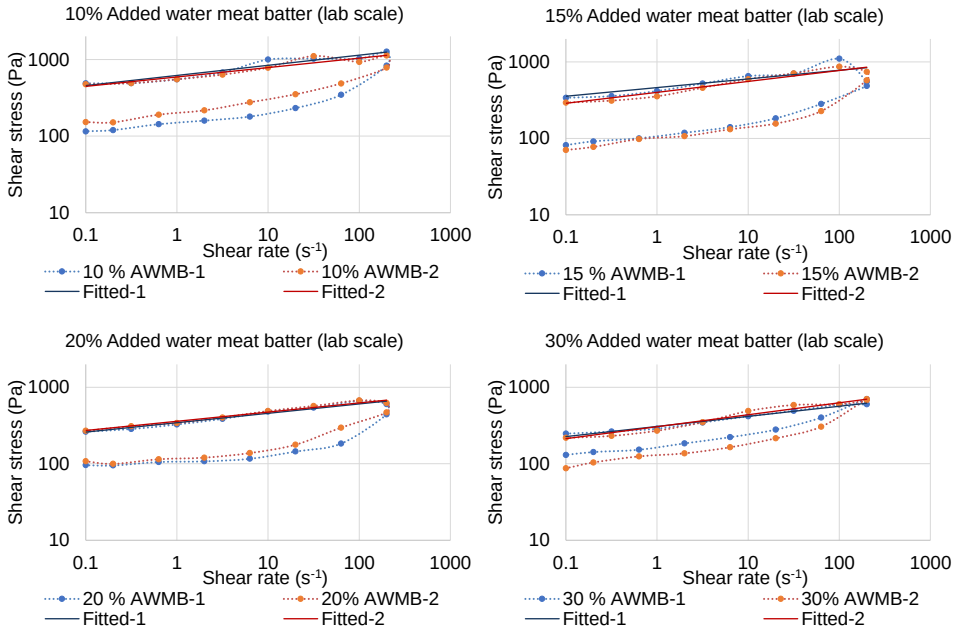


**Figure 26 Flow curve of laboratory scale meat batter with upward sweep fitted line to Power Law equation**

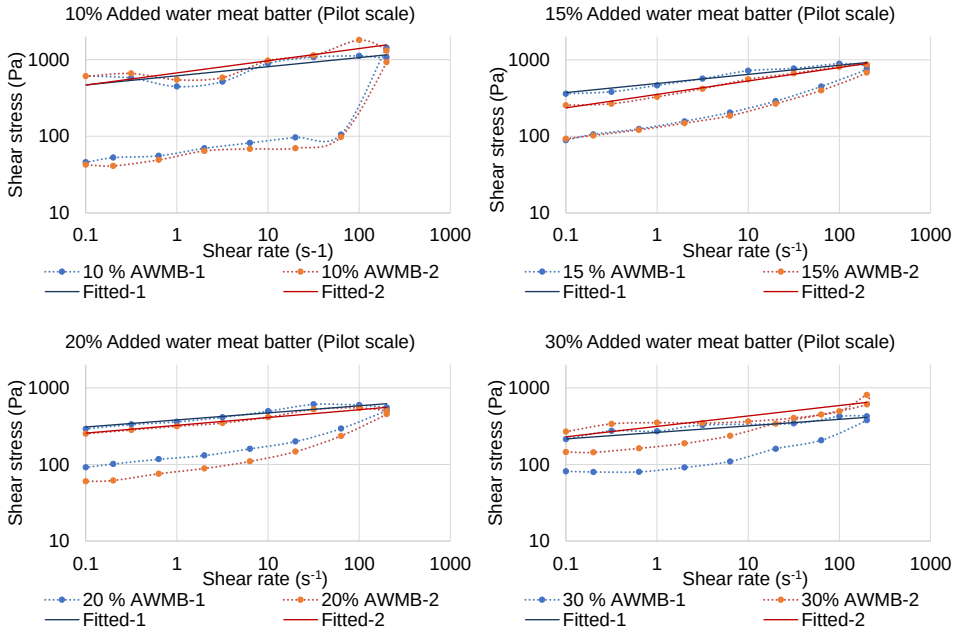


**Figure 27 Flow curve of pilot scale meat batter with upward sweep fitted to Power Law equation**

## 4.1.2 **Meat Batter Rheological Parameters**

The Power Law model Equation (3) was used to calculate the rheological parameters K-value and n value from the rheograms presented as tabulated below. The Ordinary Least Square Method was used to determine the fitted curve of the models. Only the sweep up was considered for the rheological parameter because the data gained from that range of shear rate were more reliable and applicable for the filling process in TPR2 machine. Table 4 shows the rheological parameters of the meat batter.

**Table 4 Rheological Parameters, K and n values of Meat Batters**

| | ***K value (Pa-s)*** | | ***n value*** | |
|---|---|---|---|---|
| ***% Added water to meat batter*** | ***Laboratory*** | ***Pilot Plant*** | ***Laboratory*** | ***Pilot Plant*** |
| 10 | 605±14$^{a}$ | 644±27$^{a}$ | 0.14±0.02$^{a}$ | 0.14±0.02$^{a}$ |
| 15 | 431±30$^{b}$ | 422±68$^{b}$ | 0.15±0.03$^{a}$ | 0.15±0.03$^{a}$ |
| 20 | 352±7.4$^{b}$ | 352±28$^{b}$ | 0.12±0.00$^{a}$ | 0.10±0.0$^{a}$ |
| 30 | 306±1.0$^{c}$ | 288±26$^{c}$ | 0.15±0.015$^{a}$ | 0.12±0.020$^{a}$ |

*Means within each column and across the row for K value and n value with the same letter are not significantly different (p>0.05)

*4.1.2.1 K value*

It could be observed that there is a decreasing trend of K value as the water added increases. As seen in Figure 28, the K values range from 288-644 Pa-s. There was no significant difference ($p>0.05$) between the laboratory samples and the pilot plant scale samples. The 15% AWMB did not differ from that of 20% but both were significantly different with 10% and 30% AWMB.

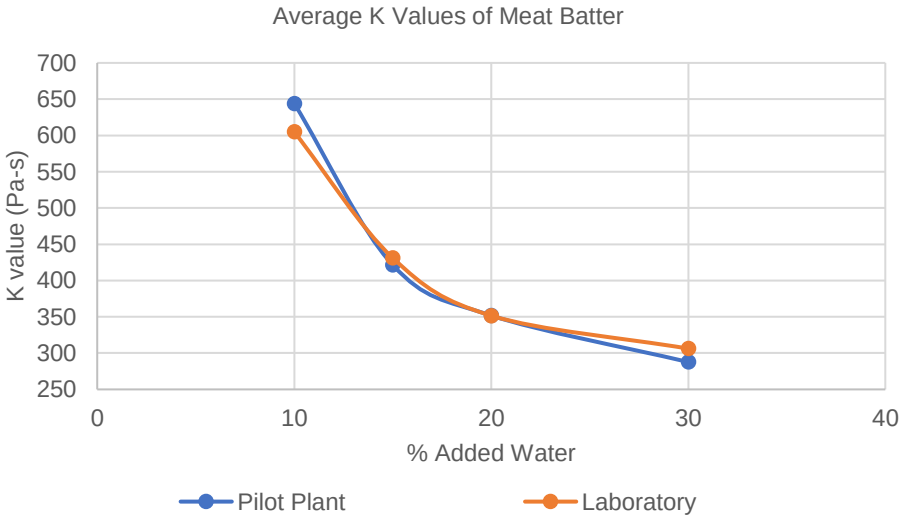


a

**Figure 28. Average K Values for Laboratory and Pilot Plant Scale AWMB**

Toledo, Cabot, and Brown (1977) studied the relationship between the composition and stability of raw comminuted meat batter to its rheological properties. Formulations of varying protein (9-18%), fat (20-60%), and moisture content (30-60%) were analyzed of which no added water was done. Increase in the fat content resulted to a reduction of the resistance to flow of the batter as observed in the decrease in the K values which ranged from 14 to 858 Pa-s.

*4.1.2.2 n value*

It could be seen from the table that the n values did not significantly differ ($p>0.05$) from each other. Also, there was no clear correlation between the % added water and the n value which ranges from 0.1 to 0.15. This was in conjunction with Toledo, et al (1977) study in which the interaction between the protein, fat, and moisture content did not show any relation with the n value.

*4.1.2.3 Apparent Viscosity*

The apparent viscosity at shear rate $32s^{-1}$, $\eta_{32}$ were calculated from the Power Law model using Equation (6). At shear rate 32 $s^{-1}$, it is the sampling point on upward sweep which was close to the assumption of shear when the meat batter is in the recovery tank and stirred with agitator at 30Hz. The values for the laboratory and

pilot plant scale are tabulated below. A decreasing trend in the $\eta_{32}$ was observed for both laboratory and pilot plant scale as seen in Table 5 and Figure 29.

**Table 5 Apparent Viscosity, $\eta_{32}$**

| | *Apparent Viscosity (Pa-s) at 32s$^{-1}$* | |
|---|---|---|
| ***% Water Added to Meat Batter*** | Laboratory | Pilot Plant |
| 10 | 30±1.0[a] | 33±4.0[a] |
| 15 | 22±0.5[b] | 22±1.5[b] |
| 20 | 17±0.0[c] | 16±1.0[c] |
| 30 | 16±1.0[c] | 14±2.5[c] |

*Means within each column and across the row with the same letter are not significantly different (p>0.05)

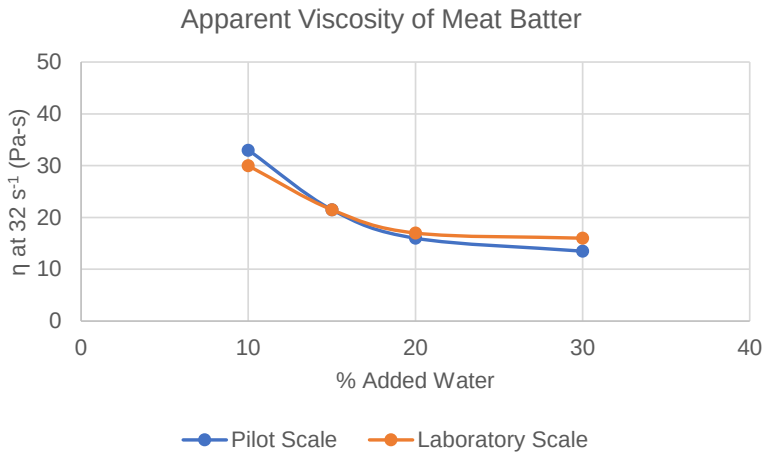


**Figure 29 Average apparent Viscosity at 32s$^{-1}$ for meat batter with different % added water**

Gorbatov and Kosoy (1970) as cited by Gorbatov and Gorbatov (1974) conducted study on the effect of moisture content, temperature, and pressure to the sausage meat properties. The increase in the water content of the formulations result to reduction of viscosity and loosening of structural links between meat particles. The study revealed that these phenomena are caused by the increase in the water interlayers between the particles and the redistribution of water due to osmosis which also result to the growth in particle size.

### 4.1.3 **Meat Batter Thixotropy Properties**

There are many tests that could be performed to explain the thixotropic property of a food matrix. One is by the obtaining the rheology flow curve of sweep up and down. Another method is conducting the breakdown and build-up test.

#### *4.1.3.1 Hysteresis Loop Difference*

Table 6 shows the percentage difference of the hysteresis loop as calculated based on Figure 24.

**Table 6 The percentage difference of hysteresis loop**

| *% Added water to meat batter* | *% Difference* | |
|---|---|---|
| | ***Laboratory scale*** | ***Pilot scale*** |
| 10 | 72±5 | 93±0.2 |
| 15 | 76±0.01 | 69±6 |
| 20 | 62±2 | 72±4 |
| 30 | 54±6 | 54±8 |

The differences of initial shear stress and final shear stress on hysteresis loop show that the different percentage of water added to the meat batter could affect the thixotropy property of the meat batter. As the water added increased, the thixotropic behavior decreased as reflected by the lower %difference. The sample with least %difference was 30% AWMB. The same trend was observed for both Laboratory scale and Pilot scale. While the highest %difference was pilot scale 10% AWMB. It had % difference of 93±0.2% which could indicate the strongest thixotropic properties amount all samples.

The shear stress presented the relationship as a function of shear rate. All samples show the flow history dependent characteristics as the sweep down lines were lower than the sweep up curves. It could be described by its thixotropic characteristic. The high shear rate applied to meat batter during the sweep up was responsible for the internal structure broken down which resulted to lower shear stress obtained during the sweep down. (Moller, Fall, Chikkadi, Derks and Bonn, 2009)

The difference in the % amount of water added to the meat batter could be the reason why the areas between curve were different. The lesser added water in the matrix translated to more lean meat with available soluble proteins that surround the fat droplets or small fat particles which create strong network that holds the water. (Lonergan et al, 2018) Therefore, the effect of more available protein, less additional water contributed to more thixotropic property.

*4.1.3.2 Breakdown Test*

The constant shear rate was applied to the samples for the break down test and the sample result is presented in Figure 30. The graphs for 15%, 20%, and 30% were presented in Appendix G. The fluctuation in the result of the break down test was observed. This could be explained by the complexity of the matrix that consists of many types of particles which is affected differently with the shear rate. (Cheng and Evans, 1965) By performing this test, the result confirmed the shear-thinning behavior of the meat batter as the declining of apparent viscosity when the shear rate is increased. The decrease of apparent viscosity could be explained by the arrangement of structural unit to the direction of flow that response to the applied shear. (Chhabra and Richardson, 2008)

Initial viscosity and the last point of sampling of break down test were used for the comparison and represented on Table 7. The difference shear rate in this study, did not affect the break down rate. And regardless of the shear rate, meat batters showed the same break down rate in general. Except for at shear rate 50 $s^{-1}$, 10%, 15% and 20% AWMB have no significant difference. While 30% AWMB was significantly different with 15 and 10% but the same with 20% AWMB.

**Table 7 The percentage of difference viscosity of break down test in %**

| | ***% Added Water to Meat Batter*** | | | |
|---|---|---|---|---|
| ***Shear rate ($s^{-1}$)*** | 10 | 15 | 20 | 30 |
| 10 | 65±6.2$^{ab}$ | 65±5.6$^{ab}$ | 59±13$^{ab}$ | 47±20$^{ab}$ |
| 50 | 62±4.1$^{a}$ | 52±2.0$^{a}$ | 48±4.2$^{ab}$ | 39±2.3$^{b}$ |
| 100 | 56±20$^{ab}$ | 62±0.16$^{ab}$ | 53±5.6$^{ab}$ | 38±13$^{ab}$ |

*Means within each column and across the row with the same letter are not significantly different ($p>0.05$)

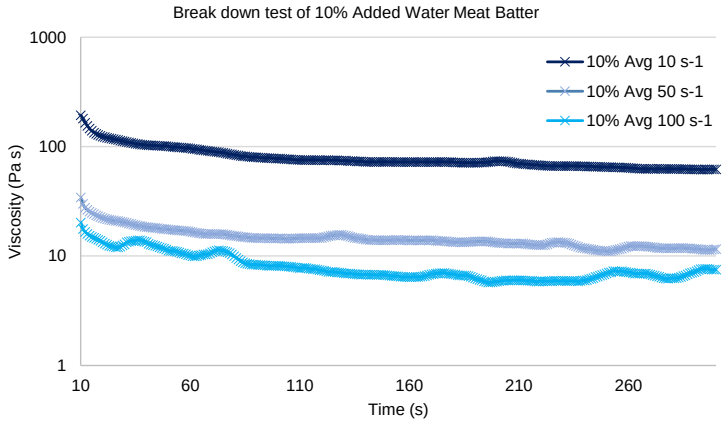

**Figure 30 Break down test for Thixotropic study of laboratory scale 10% AWMB with shear rate 10, 50 and 100 $s^{-1}$**

*4.1.3.3 Build-Up Test*

Another measurement for understanding thixotropy property was conducted, aiming to determine the difference structure recovery ability across meat batter. The graph with plotted viscosity versus time can be seen in Figure 31. The graphs for 15%, 20% and 30% can be seen in Appendix H. Presented data were captured after the pre-shearing or break down phase at high shear rate or called as the buildup phase with different resting time. In Table 8, the percentage from structural parameter were presented. They were computed by the Equation (12) and converted into percentage. The values of all samples were more than zero which mean that the structure of meat batter was recovering within the duration of study. However, the low % structural could mean that more time is needed for the meat batter to build-up. It is expected that the longer resting time, the higher percentage of structure parameter would be as the structure allowed to be recovered more. In general, the significant different of percentage of structural parameter was not observed with the different resting time. It shows that there is no significant different among 10%, 15% and 20% AWMB. However, the 30% AWMB with the longest resting time shows significant difference. With previous test on break down test showed that 30% AWMB has different thixotropic behavior compared to other meat batter sample.

The investigated resting period might not be enough to see the effect of time on build-up ability for other samples. However, the long product residence time in filling machine is not the aim for production process. Therefore, the build-up ability of meat batter could not affect the filling process with such a rapid filling duration.

**Table 8 The percentage of structural parameter of build-up test, %**

| | *% Added Water to Meat Batter* | | | |
|---|---|---|---|---|
| ***Resting Time*** | 10 | 15 | 20 | 30 |
| 0 | 3.9±0.021[a] | 4.8±0.000[a] | 4.6±0.012[a] | 6.6±0.012[a] |
| 30 | 3.9±0.021[a] | 4.6±0.035[a] | 5.0±0.002[a] | 17.2±0.016[a] |
| 90 | 3.9±0.021[a] | 7.1±0.012[a] | 5.5±0.007[a] | 3.8±0.001[a] |
| 300 | 3.9±0.021[a] | 3.0±0.038[a] | 9.3±0.034[a] | 26.8±0.018[b] |

*Means within each column and across the row with the same letter are not significantly different ($p>0.05$)

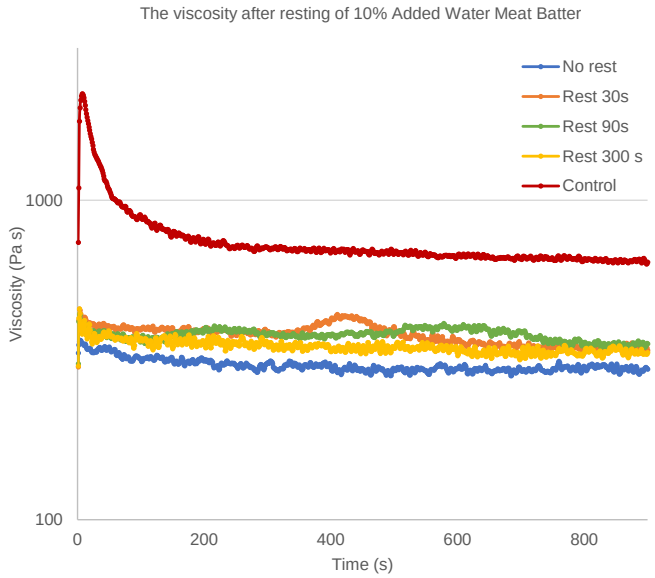


**Figure 31 The buildup test shown the structure recover after resting time (0, 30, 90 and 300 s) of laboratory scale 10% AWMB**

### 4.1.4 **Meat Batter Viscoelastic Properties**

The viscoelastic property 15% and 20% AWMB was studied using the amplitude sweep. Figure 32 and 33 show the graphs of the elastic modulus, viscous modulus, and phase angle against the shear stress range from 1-1000Pa at a constant frequency of 1 Hz at 10°C. The elastic modulus, G' for both meat batter at lower shear stress were higher than the viscous modulus, G" which means that the elastic part is more dominant which is expected as meat batter behaves like solid due to the complex interaction among its fat, protein, fiber, and water content.

As the shear stress was increased, the G' and G" for both meat batters decreased but with the faster rate for 20% AWMB. The average critical stress, $\sigma^*$ at which the G' had the same value as G" or when the phase angle became 45° was at 1000Pa and 742±74Pa for 15% and 20%, respectively. At this specific stress, the meat batter elastic and viscous properties were equal which could mean that the product could start to flow.

The Force contribution, F* force exerted by the meat batter to the pipe was computed by multiplying $\sigma^*$ with the area of the pipe:

$$F^* = \sigma^* Area_{pipe} \tag{22}$$

of which the area of the pipe is calculated by:

$$Area_{pipe} = Length * radius *\pi \tag{23}$$

The pressure drop (elastic contribution) caused by the stress contribution of the meat batter to the pipe was calculated using the following formula:

$$\Delta P_{elastic\ contribution} = \frac{F^*}{Cross\ section\ Area_{pipe}} \tag{24}$$

The stress contribution was computed based on Equation (27) along the pipe were 51N and 44N for 15% and 20%. These values were then converted to the elastic ΔP contribution of the meat batter as it moved along the pipe based on Equation (29) which were 261hectoPa (hPa) for 15% and 193hPa for 20% AWMB of which 1hPa is equal to 100Pa.

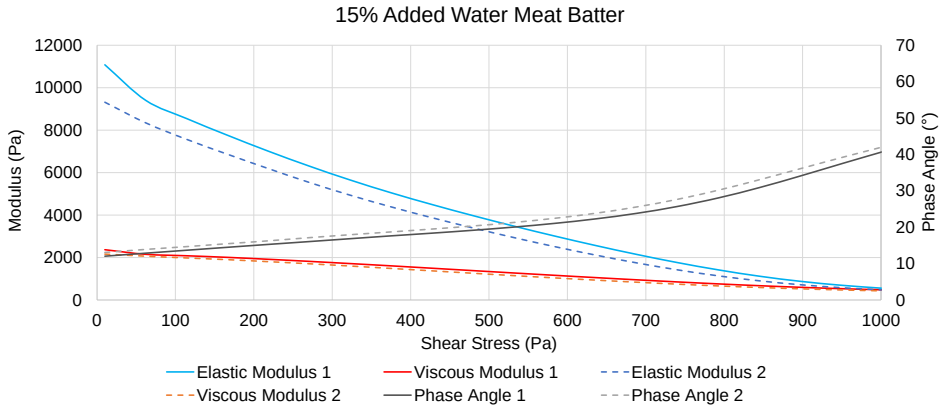


**Figure 32. 15% Added Water Amplitude Sweep**

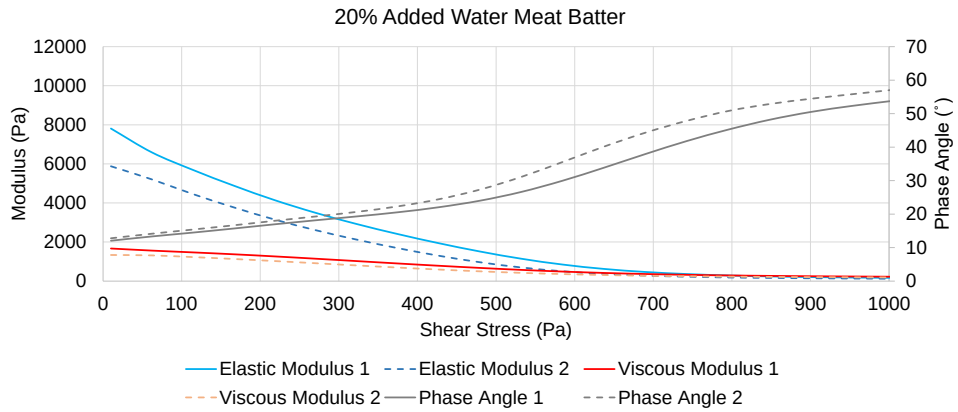


**Figure 33. 20% Added Water Amplitude Sweep**

## 4.2 Meat Batter Machine Test

Four different meat batter with varying amount of water were tested in the TPR2 Machine. This was done to see the behavior of the different meat batter with different rheology, fillability and viscoelastic properties brought about by the changes in the added water. The 30% and 10% AWMB were tested consecutively in one day while the 20% and 15% were tested on separate day due to the availability of the machine. The data generated in this experiment were pressure measurements P1 (nearest the tank) and P2 (nearest to the piston) as seen in Figure 14. The pressure drop, ΔP was calculated by getting the difference between P1 and P2.

The TPR2 Machine was able to fill both the 20% and 30% AWMB as seen in the Figure 34. On the other hand, 10% and 15% AWMB were not able to be filled by the machine.


**Figure 34 Filled packaged with pilot scale meat batter a) 10% AWMB, b) 15% AWMB, c) 20% AWMB and d) 30% AWMB**

### 4.2.1 **Meat Batter Pressure Profile Curves**

Piston filler works by the intake stroke of the filler which draws out the meat batter from the tank. (Hughes, 2007) This movement creates a pressure difference, ΔP that results to the flow of the meat batter which is the focus of this study.

#### *4.2.1.1 30% AWMB*

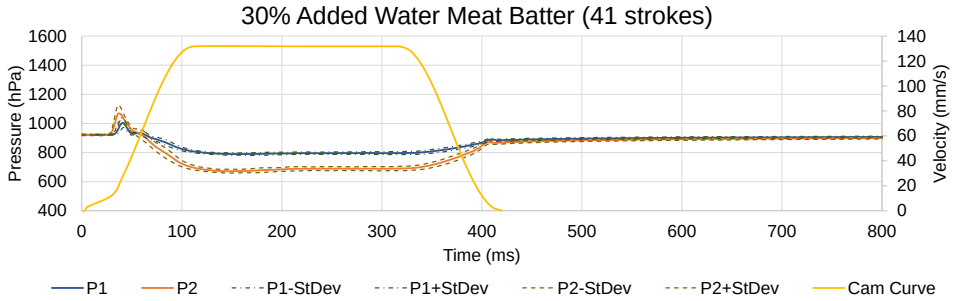


**Figure 35 Pressure Profile Curve 30% AWMB**

Figure 35 shows the pressure profile curve for 30% AWMB for 41 strokes during the whole filling process. This meat batter was able to flow through the pipe and be filled by the TPR2 machine. As the valve opened, no pressure difference was observed not until 20ms when the piston started moving and accelerating. A rapid and significant increase in the P2 and P1 was observed. This brought pressure gain in the system which may be due to the opening of the valve which exerted pressure to the meat batter, resulting to sudden back flow. This could mean that the piston cylinder has high pressure build-up inside as seen in Figure 36. As the piston accelerated, the P2 pressure values decreased significantly as compared to P1. As the piston moved at its maximum and constant speed of 132mm/s, plateau pressure values or defined as steady state was observed in which there was no significant change in the pressure measurements. At this duration, the pressure drop was constant which could mean that the meat batter then started to flow and fill the piston

chamber as the piston moved to a specific distance corresponding to the desired volume.

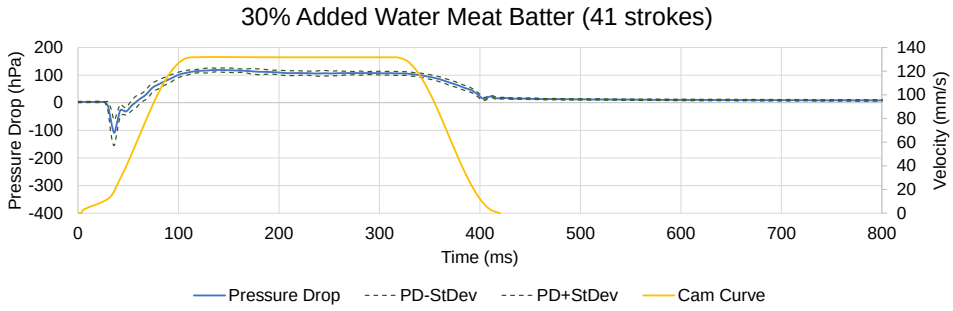


**Figure 36 Pressure Drop Curve 30% AWMB**

Beynart (2009) explains that during the suction stroke, the piston movement away from the head reduces the pressure in the cylinder. Since there is atmospheric pressure on the surface of the meat batter, the difference in the pressure forces the meat batter to flow through the pipe until the piston cylinder. Gorbatov and Gorbatov (1974) explained the behavior of sausage meat batter under stress. With the very low stress, the batter behaves like solid with permanent deformation. As the amount of stress is increased, meat batter is observed to result to have resilient aftereffect which may yield to creep or permanent deformation. As the limit or yield stress is approached, the meat batter structure breaks down partially leading to viscoplastic flow which is described by the highest effective viscosity (EV) Gorbatov and Kazakov (1959) as cited by Gorbatov and Gorbatov (1974).

As the piston decelerated, the P2 pressure increased significantly as compared to P1. A small increase in the pressure drop was observed as seen in Figure 36 as the piston stopped and the valve was closed. The pressure drop returned back to zero as there was no flow in the pipe. The zero pressure drop lasted until the start of the next stroke.

*4.2.1.2 20% AWMB*

Figures 37 and 38 show the pressure profile and pressure drop of 20% AWMB, respectively. The initial pressure values were higher compared to that of 30% AWMB. It could also be observed the significant increase in the pressure values as the valve was opened and the piston started to accelerate as also seen in 30% AWMB. However, the increase in the pressure values was lesser than that of the 30% AWMB. During the acceleration of the piston, P2 maintained to be greater than P1 which resulted to the pressure gain of the system. This could mean that the opening of the valve yielded to the added pressure to the meat batter, coming from the piston. Since the 20% AWMB has more elastic property than the 30% AWMB, it has more tendency to store the energy, thus prolonging the pressure gain in the system. As the piston accelerated to its maximum velocity, only then the pressure

values decreased. This resulted to the delay in the steady state region in which there was a steady flow of the meat batter.

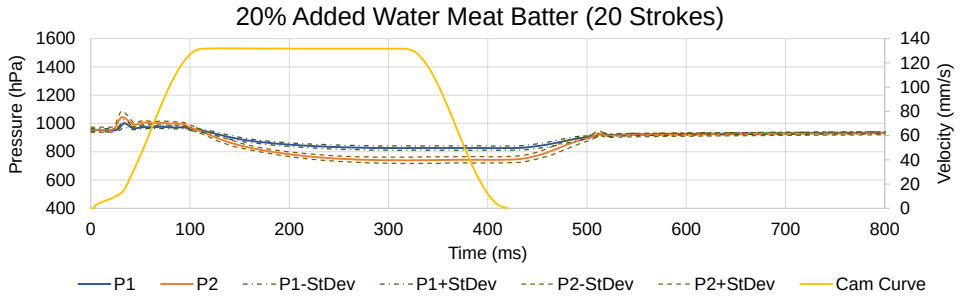


**Figure 37 Pressure Profile Curve 20% AWMB**

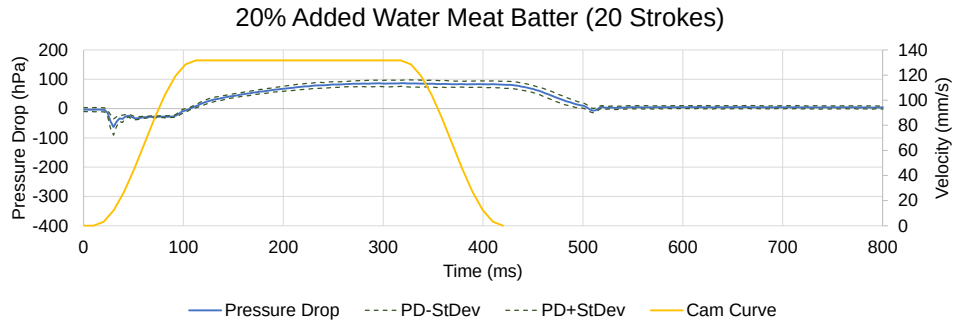


**Figure 38 Pressure Drop Curve 20% AWMB**

The difference in the pressure profile and pressure drop curves between 30% and 20% AWMB even if they were both able to be filled in the machine is may be due to their thixotropy properties. Moisés, Alencar, Naccache, and Frigaard (2018) conducted the study to determine the effect of the thixotropy effect of different suspensions during a pipe flow which were Carbopol® and Laponite® which are non-thixotropic and thixotropic, respectively. Suspensions with less thixotropy property tend to attain steady state faster as compared to incompressible thixotropy suspension. The rheological flow curves as presented in Figure 27 and 28 showed that 30% AWMB had less thixotropy property than 20% AWMB, thus it was able to attain the steady state region faster. As the piston decelerated, the pressure drop had still attained constant value which could mean that there was still steady flow. The stopping of the piston movement and closing of the valve resulted to increase in the pressure values and reduction of pressure drop. Only after 500ms that the pressure drop value returned to zero which could mean that the elastic property of the meat batter was causing the change in the pressure measurements.

*4.2.1.3 15% AWMB*

The 15% AWMB was not filled properly in the packages but only fill 25% of the volume required. Figure 39 and 40 show the pressure profile and pressure drop curves, respectively. It could be observed that the initial pressure measurements were lower as compared to those of 30% and 20% AWMB. The possible reason for this was that the pipe was not fully filled with the meat batter which reduced the pressure exerted to the pipe. As the valve was opened and the piston started to accelerate, the P2 increased significantly with the magnitude increase more than those of 30% and 20% AWMB. This could mean that more pressure was stored in the piston causing more impact to the backflow of the meat batter in the pipe.

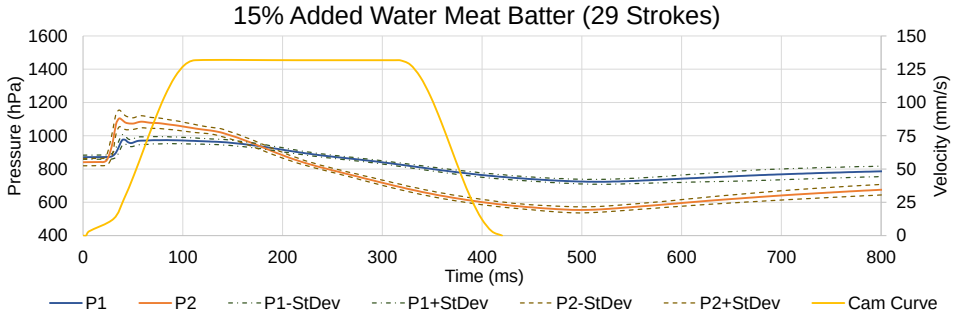


**Figure 39 Pressure Profile Curve 15% AWMB**

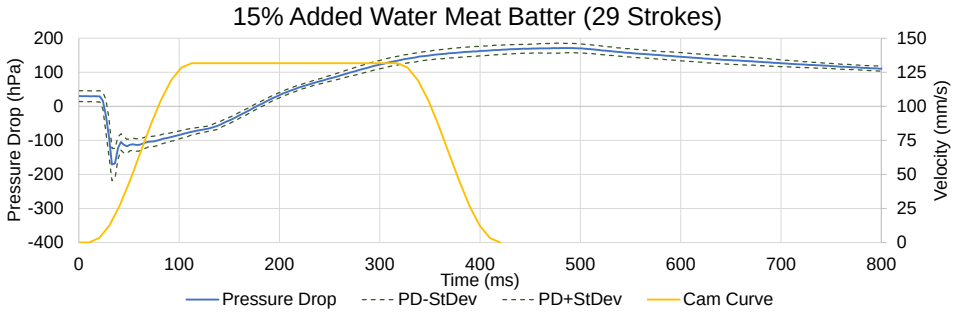


**Figure 40 Pressure Drop Curve 15% AWMB**

Since the pressure gained as the valve was opened was relatively higher, it took longer time for the pressure to decrease even if the piston has already reached its maximum constant speed. Only until 200ms that the P2 became lower than P1 which meant that the steady flow was about to start. As the piston continued to move at maximum speed, the pressure values decreased significantly which resulted to the increase in the pressure drop. However, the movement of the piston was not enough to achieve the steady state or the steady flow of the meat batter. Even after the valve was closed, a significant pressure drop was still observed which meant that there was still a flow along the pipe. This could be explained by the elastic property of the 15% meat batter and that the pressure drop created by the piston movement was

not enough for the meat batter to flow. Even if there was no piston movement and the valve was closed, a slow increase in the pressure values were recorded.

Fyodorov and Gorbatov (1960) as cited by Gorbatov and Gorbatov (1974) studied the sausage meat batter flow through the set-up of polyethylene pipes with diameter 0.014-0.050m, piston stuffer, and X-ray apparatus. Three general pattern of velocity distribution were observed during the study: (1) adherence of thin layer of dispersed material on the wall (2) layer of flowing mass (3) solid-like center but slightly deformed plug. This might occur with the 30% and 20% AWMB in which both had the flow and the packages were able to be filled. However, for 15% AWMB, a significant amount of dispersed amount of material may have adhered to the walls of the pipe. Thus, only small amount of meat batter was able to flow as more force was needed to be exerted in order to fill the packages with the proper volume.

*4.2.1.4 10% AWMB*

Figure 41 and 42 show the pressure profile and pressure drop curves for 10% AWMB. The same trend for increasing P2 as the piston started to accelerate was observed with 10% AWMB and was significantly the highest among all the meat batter samples. This could mean that there was very high-pressure build-up in the piston cylinder. This resulted to slow decrease of P2 as the piston accelerated. As the piston reached the maximum constant velocity, the ΔP became positive and continued to increase as the piston was moving to pull the product inside the cylinder. This could mean that there was a flow in this instance. The shift from pressure gain (-ΔP) to positive ΔP was faster than that of 15% AWMB. The increase in the pressure drop stopped as the valve was closed, and as the piston stopped moving. A very gradual decrease in the ΔP which did not change significantly was observed until it reached to the average zero ΔP.

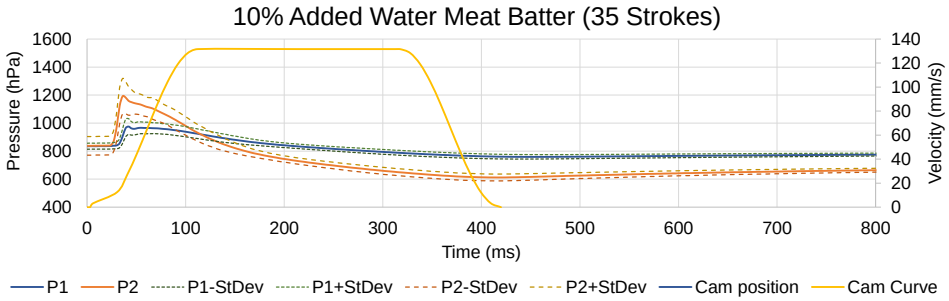


**Figure 41 Pressure Profile Curve 10% AWMB**

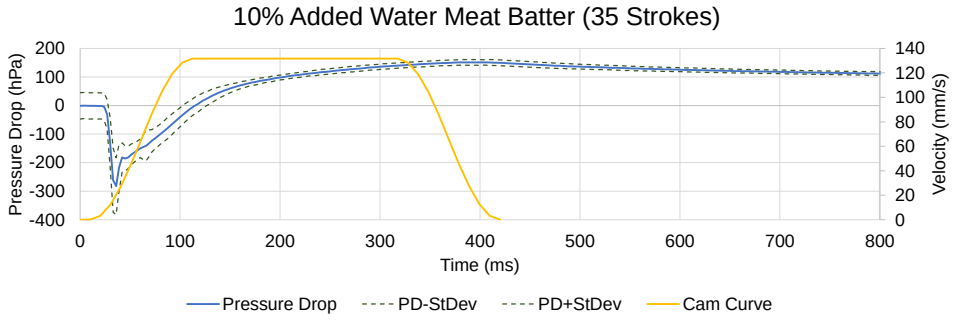


**Figure 42 Pressure Drop Curve 10% AWMB**

As discussed in the previous section, the pressure profile curves differ among the meat batter samples. Figure 43 below shows the different sections that were used to compute for the average experimental ΔP. The different sections include (Section A) at which the piston was at it constant and maximum velocity, (Section B) at which the pressure measurements do not change significantly or when the ΔP was constant (steady state), and (Section C) after constant piston velocity or when the piston started decelerating, at 320ms until 520ms.

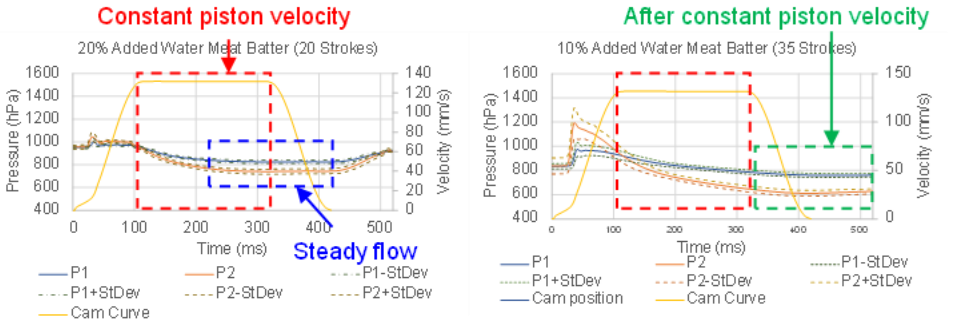


**Figure 43 Different regions in the Pressure Profile Curves**

It was observed that 30% AWMB exhibited the same Section A and B as its steady state was the same as when the piston was at constant velocity, giving the value 110±4.4hPa as tabulated in Table 9.

On the other hand, 20% had delayed steady state region which lasted until the piston stopped and the valve was closed. Thus, the average ΔP at section A and B were calculated which were 65±22hPa and 84±1.3hPa, respectively. The high standard deviation in section A (34%) could mean that the ΔP has not reached its steady state and was still increasing during the time at which the piston was at constant velocity. On the other hand, calculating for the ΔP at Section B for 20% AWMB gave significantly low standard deviation (1.5%) which could mean that a steady flow occurred at this duration. The 20% AWMB was lower in ΔP than that of 10% AWMB in both Sections A and B.

For 10% and 15% AWMB, the steady state region was not observed when the piston was at constant velocity. With the cam curve setting in this study, it may limit the flow development with higher pressure drop that could happen in longer time as the delay tends to occur as additional water is decreased. The values for Section A for 10% and 15% AWMB were 91±40hPa and 38±67hPa, respectively. The high standard deviation showed that there was still significant change in the pressure values at this duration, which is more evident with 15%. It was also noted that the ΔP for 10% AWMB was higher than that of 15% AWMB. This could mean that higher pressure drop was needed to make the 10% AWMB flow during the start of the suction process. Also, ΔP at section C were computed and had the values of 144±5.5hPa and 162±10hPa, respectively. The 10% AWMB was lower than that of 15% AWMB at Section C. However, since the TPR2 machine was not able to fill these meat batter, the ΔP for the 15% and 10% AWMB was caused by the presence of mixture of air and meat batter in the pipe. The piston filler was able to fill the package at 6% (w/v) for 10% AWMB as compared to 25% (w/v) for 15% AWMB which could be the reason for such disparity.

**Table 9 Average Experimental Pressure Drop of Meat Batter**

| *% Added Water to Meat Batter* | *Pressure Drop (hPa)* | | |
|---|---|---|---|
| | Piston at Constant Velocity | Steady State | After Piston at Constant Velocity |
| 10 | 94±39 | - | 144±5.5 |
| 15 | 38±67 | - | 162±10 |
| 20 | 65±22 | 84±1.3 | - |
| 30 | 110±4.4 | 110±4.4 | - |

This information could be used in designing the set-up of the filling machine especially for high viscous product like meat batter. Henry (2020) emphasized the importance of placing the reservoir above the filling nozzle to provide positive inlet head to the piston. It is also important that the inlet head pressure remains constant.

## 4.3 Correlation of Pressure Profile Curves and Rheology

The calculated pressure drop values from the calculation using the Power law were compared with the experimental pressure drop.

### 4.3.1 **Calculated Pressure Drop**

The estimated ΔP was calculated for different meat batters produced in laboratory and pilot plant using the calculated K and n values from Power Law model derived from Hagen poiseuille equation with Rabinowitsch-Mooney correction factor Equation (21) from shear rate 0.1 to 200 $s^{-1}$. The L used was the length of the pipe between the inlet pipe (P1) and the area in the pipe near the piston (P2). The flow rate, Q was derived from the velocity of the piston and the area of dosage cylinder. A decreasing trend was observed as the % amount of needed water was added to the meat batter. However, increasing the added water from 20% to 30% did not result to significant difference as seen in Table 10. This trend was also seen in the Apparent viscosity that there was no significant difference between the two meat batter samples. It was also notable the relatively high ΔP for 10% and 15%. The calculated pressure drop across all the % Added water did not significantly differ between laboratory and Pilot plant data. This could mean that the laboratory preparation and sampling method could be used to represent the Pilot plant scale.

**Table 10 Calculated Pressure Drop***

| | ***Calculated Pressure Drop (hPa)*** | |
|---|---|---|
| ***% Added water to Meat Batter*** | Laboratory | Pilot Plant |
| 10 | 204±15[a] | 219±30[a] |
| 15 | 152±11[b] | 147±3.3[b] |
| 20 | 108±2.3[c] | 98±7.8[c] |
| 30 | 106±7.1[c] | 89±16[c] |

*Means within each column and across the row with the same letter are not significantly different ($p>0.05$)

### 4.3.2 **Comparison of Experimental and Calculated Pressure Drop**

Table 11 below shows the comparison of the experimental from Table 9 and calculated pressure drop values from Table 10. The equation used for the % relative difference was:

$$\%\ Relative\ Difference = \frac{(\Delta P_{calculated} - \Delta P_{experimental})}{\Delta P_{experimental}} x100 \qquad (25)$$

It was observed that the Power Law underestimated the 30% AWMB by 4-24%. However, overestimation from 16-75% was observed with lower % AWMB. This could mean that the Power Law model only fitted well with higher % added water to the meat batter. The result shows that the Rabinowitz-Mooney equation for Power Law model is not good fit to predict meat batter with % added water lower than 30%.

**Table 11 % Relative Difference of Pressure Drop***

| *% Added Water to Meat Batter* | *Experimental (Piston at Constant Velocity)* | | *Experimental (Steady State/After Constant Velocity)* | |
|---|---|---|---|---|
| | Calculated (Pilot Plant) | Calculated (Laboratory) | Calculated (Pilot Plant) | Calculated (Laboratory) |
| 10 | 57.1 | 53.9 | 52.1 | 41.7 |
| 15 | 74.1 | 75.0 | -9.3 | -6.2 |
| 20 | 33.7 | 39.8 | 16.7 | 28.6 |
| 30 | -23.6 | -3.8 | -19.1 | -3.6 |

*Negative value means underestimation of Power Law model

### 4.3.3 **Extrapolated Pressure in the Piston**

Based on the rheological parameters computed using the Power Law model and by the Rabinowitsch-Mooney equation for pressure drop, the pressure at the piston's maximum length during suction was extrapolated.

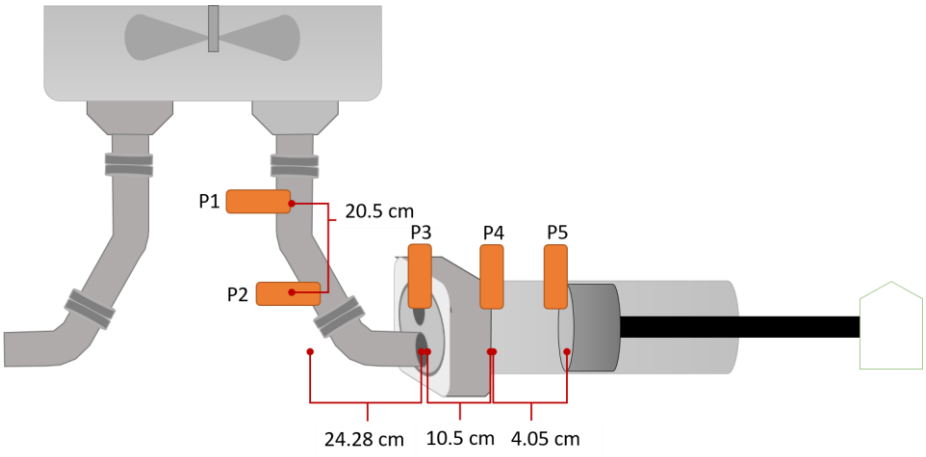


**Figure 44 Simplified version of TPR2 Machine with different sections for extrapolation**

The estimated ΔP from the P1 up to the piston was calculated by computing for the estimated pressure drop within different sections as seen in Figure 44. The estimated $\Delta P_{P1\text{-}P2}$ was calculated using Equation (21). This value was used to compute for the pressure at the valve, P2 using following equation:

$$P2 = P1 - \Delta P_{P1-P2} \tag{26}$$

by using the length from P1 to P2 as L. The estimated $\Delta P_{P2\text{-}P3}$ was calculated using the same equation and the L used was from P2 until the valve. The P3 was then computed with the formula:

$$P3 = P2 - \Delta P_{P2-P3} \quad (27)$$

Using the Equation (27), the estimated $\Delta P_{P3\text{-}P4}$ was calculated with the length from opening of the valve up to the opening of the piston cylinder. Then, the P4 equation used was:

$$P4 = P3 - \Delta P_{P3-P4} \quad (28)$$

The estimated $\Delta P_{P4\text{-}P5}$ was computed using L as the distance of movement of the piston during the suction. Of which the P5 was calculated by:

$$P5 = P4 - \Delta P_{P4-P5} \quad (29)$$

The $\Delta P_{P1\text{-}P5}$ was calculated by the difference of the experimental P1 and calculated P5.

$$\Delta P_{P1-P5} = P1 - P5 \quad (30)$$

Table 12 shows the extrapolation of the Pressure drop based on Equation (30) and absolute pressure at piston based on Equation (29) for the different meat batter. As the added water content increased, the extrapolated absolute pressure increased and the pressure drop decreased. Also, this low pressure in the piston for 10% water added, resulted to relatively high pressure drop at 636hPa and 739 hPa for laboratory and machine, respectively. Zero absolute pressure could mean that the vacuum may be developed inside the piston. (Rajput, 2005) The temperature of the meat batter was maintained at 10°C and based on the steam table, water boils at 10°C when the pressure is 12 hPa. (Koretsky, 2013) Assuming that the piston was able to reach below 12hPa in order to fill the cylinder with 10% AWMB, steam might have formed in the piston due to the boiling of the water molecules in the meat batter. This will create problem in the filling process. This problem might not occur with 15% AWMB since the boiling point of water at 280hPa-300hPa is 65°C. (Koretsky, 2013) This extrapolation described the limitation of the TPR2 machine to fill viscous materials such as 10% AWMB due to the low extrapolated pressure in the piston.

**Table 12 Extrapolation of Absolute Pressure and Pressure Drop from the Piston**

| *% Water added to meat batter* | *Extrapolated Absolute Pressure at Piston, P5 (hPa)* | | *Extrapolated Pressure Drop from experimental P1 to piston (P5) (hPa)* | |
|---|---|---|---|---|
| | *Laboratory* | *Pilot Plant* | *Laboratory* | *Pilot Plant* |
| 10 | 114 | 11 | 636 | 739 |
| 15 | 282 | 300 | 517 | 498 |
| 20 | 472 | 508 | 360 | 324 |
| 30 | 398 | 496 | 397 | 299 |

Using extrapolated pressure drop from P1 to piston as the elastic contribution and the viscous ΔP contribution from the amplitude sweep, the total pressure necessary for the meat batter to flow from the tank up to the piston, assuming with correct volume, was calculated. The total ΔP needed for the product to flow was computed by determining the sum of the $\Delta P_{P1\text{-}Piston}$ from 3.3.3.2. and $\Delta P_{\text{ elastic contribution}}$.

$$Total\ \Delta P = \Delta P_{P1-Piston} + \Delta P_{elastic\ contribution} \quad (31)$$

The calculated total pressure drop for 15% added water meat batter was 759hPa while it was 517hPa for 20% of which approximately more than 30% is caused by the elastic contribution. Thus, it could be inferred that the elastic property of the meat batter contributed significantly to the stress contribution of the meat batter during the flow.

# 5 Conclusion

*This section includes the summary of the conclusions made from this study.*

1. The rheological characteristics of the meat batter could be studied using the vane geometry in the rotational rheometer which showed that the meat batter could be described by the Power Law Model. The rheological measurements provide K and n values of which the former decreased as the % added water was increased, while the latter was not significantly affected. Shear thinning behaviour was observed among all the samples. The calculated apparent viscosity and pressure drop estimated from the rheological measurements showed decreasing trend as the % added water was increased.

   The calculated K value and amplitude sweep test can be used to predict the meat batter's fillability in the filling machine with a standard tank and when to recommend the filling machine with pressurized tank.

   The values obtained from products produced in laboratory and pilot plant scale were not significantly different from each other.

2. The analysis of the flow curve could be used to study the thixotropy property of the meat batter which showed decreasing trend with the additional water. The filling duration is shorter than the time needed for the meat batter with lower %added water to build-up. The amplitude sweep test showed that the sample with lower water had more elastic properties.

3. The pressure measurements during the filling in the machine showed the difference in the typical pressure profile curves for products with different fillability. The meat batters which were able to be filled in the TPR2 machine with standard product tank were 20% and 30% added water meat batter that followed the viscous fluid behavior. This showed the limit of the machine without a pressurized product tank as no less than 20% added water. However, samples of 15% and 10% added water meat batter were not able to be filled exhibited more elastic property during the filling process.

4. The Rabinowitz-Mooney derived from the Power Law model used to predict the pressure drop of the meat batter samples was only applicable to 30% AWMB.

5. The fillability of the meat batter was significantly affected by its elastic property. The calculated pressure inside the piston for lower added water samples was found to be at the pressure in which water molecules could boil at 10°C which could create steam inside the piston. In addition, the mixture of meat batter and air in the pipe might have affected the filling behavior of the samples.

# 6 Recommendations for Future Research

*This section includes the recommendations for further study.*

1. Meat batter products can be further investigated in terms of viscoelastic properties and adhesiveness/stickiness by Texture Profile Analysis. This is to further understand its behaviour and to study the possibilities to correlate to its behavior during filling.

2. The fat, protein and quantitative analysis of the meat particle size can be done to determine the effect of the meat composition and microstructure on its rheological properties. The effect of varying the fat content of the meat batter can also be studied and be correlated to its fillability in the machine, to know the applicability of the prediction model in different conditions.

3. More parameter of machine response could be studied to understand how the machine works and responds to the product. This may include the motor response, synchronization to the piston movement, and the pressure measurement in the piston.

4. Study of other fluid flow models including the elastic properties could be done to determine the best fit prediction model for the meat batter with lower added water.

5. To provide a substitute for meat batter in the machine test, further study in the proxy product could be performed such as build-up, breakdown and amplitude sweep in order to compare to the rheological properties of meat batter. Machine test of the proxy product could be made in order to gather pressure data measurements and to increase the understanding of machine fillability in a systematic way.

# References


Anton Paar, (2020). Amplitude Sweeps. Retrieved May 28, 2020, from https://wiki.anton-paar.com/no-en/amplitude-sweeps/

Ahmed, J., & Ramaswamy, H. S. (2007). Dynamic rheology and thermal transitions in meat-based strained baby foods. *Journal of food engineering*, 78(4), 1274-1284.

Aktaş, N., & Genccelep, H. (2006). Effect of starch type and its modifications on physicochemical properties of bologna-type sausage produced with sheep tail fat. *Meat Science*, *74*(2), 404-408.

Allais, I. (2010). Emulsification. Toldrá, F. *Handbook of meat processing*. (pp. 143-168). Iowa: Wiley-Blackwell.

AZO Materials. (2020). Common Yield Stress And Rheological Measurement Systems. Retrieved May 15, 2020, from https://www.azom.com/article.aspx?ArticleID=9930

Barbut S. (1999) Advances in Determining Meat Emulsion Stability. In: Xiong Y.L., Chi-Tang H., Shahidi F. (Eds.), *Quality Attributes of Muscle Foods*. Boston, MA: Springer. https://doi.org/10.1007/978-1-4615-4731-0

Beynart, L. (2009). Pulsation Control for Reciprocating Pumps. McAllister, E. *Pipeline Rules of Thumb Handbook: A Manual of quick, accurate solutions to your everyday pipeline problems*. (pp. 465-472) Massachusetts: Elsevier

Chhabra, R. and Richardson, J. (2008). *Non-Newtonian Flow and Applied Rheology. Engineering Applications*. London, United Kingdom: Elsevier.

Chhabra, R. and Richardson, J. (1999). *Non-Newtonian Flow in the Process Industries: Fundamentals and Engineering Applications*. Okford, United Kingdom:Elsevier.

Cheng, D. C., & Evans, F. (1965). Phenomenological characterization of the rheological behaviour of inelastic reversible thixotropic and antithixotropic fluids. *British Journal of Applied Physics*, *16*(11), 1599. https://doi.org/10.1088/0508-3443/16/11/301

Crow. (2015). Flow properties of polymers:Time-independent fluids Retrieved May 2, 2020, from https://polymerdatabase.com/polymer%20physics/Viscosity2.html

Deshpande, A., Krishnan, J., and Kumar, S. (2010). *Rheology of Complex Fluids*. New York: Springer

Devatkal, S.K., Manjunatha, M., Narsaiah, K. and Patil, R.T. (2014). Evaluation of quality characteristics of chicken meat emulsion/nuggets prepared by using different

equipment. *Journal of food science and technology*, *51*(3), 511-518. https://doi.org/10.1007/s13197-011-0518-6

Dogan, H., & Kokini, J. L. (2006). Rheological properties of foods, Chapter 1. *Handbook of food engineering* (2nd ed.) Heldman, D.R. and Lund, D.B. (Eds.). (pp. 13-136). New York: CRC Press.

Ebrahim, H., Balla, S., & Rudge, J. (2019). Behaviour of Fluids. Maths, Physics and Clinical Measurement for Anaesthesia and Intensive Care, 53.Farmer, N. (2013). *Trends in Packaging of Food, Beverages and Other Fast-Moving Consumer Goods (FMCG): Markets, Materials and Technologies.* Cambridge, UK: Woodhead Publishing Ltd.

Gokhale, B.V. (2011). Rotary Drilling and Blasting in Large Surface Mines. NorthWestern: CRC Press

Gorbatov, A. V., & Gorbatov, V. M. (1974). Advances in sausage meat rheology. *Journal of Texture Studies*, *4*(4), 406-437. https://doi.org/10.1111/j.1745-4603.1974.tb00855.x

Henry, J. (2020). Piston Fillers. Retrieved May 11, 2020, from http://www.frainintegration.com/piston-fillers.pdf

Hoogenkamp, H. W. A. P. (2011). Protein performance in emulsion stability. *Fleischwirtschaft Int*, *3*(54), 56-59.

Honikel, K. O. (2010). Curing. Toldrá, F. *Handbook of meat processing*. (pp. 125-141). Iowa: Wiley-Blackwell.

Huang, P., Li, Y., Summer, M. (2012). Handbook of Soil Sciences: Properties and Processes (2nd ed.) New York: CRC Press

Hughes, A. (2017). Food Packaging Machinery, Chapter 22. Kutz, M. Handbook of farm, dairy, and food machinery. (pp. 698-699). Dordrecht, Netherlands: Springer

Hui, Y. (2012). *Handbook of Meat and Meat Processing* (2nd ed.) NW: CRC Press.

India Mart. (2020). Kinexus Pro+ Rheological Rheometer. Retrieved May 25, 2020, from https://www.indiamart.com/proddetail/kinexus-pro-rheological-rheometer-6450004230.html

Irgens, F. (2014) Rheology and Non-Newtonian Fluids. Cham, Switzerland:Springer

Kang, Z. L., Li, B., Ma, H. J., & Chen, F. S. (2016). Effect of different processing methods and salt content on the physicochemical and rheological properties of meat batters. *International Journal of Food Properties*, *19*(7), 1604-1615. https://doi.org/10.1080/10942912.2015.1105819

Keeton, J. T., S. M. Ellerbeck, and MT Nunez de Gonzalez. (2014) "Chemical and physical characteristics of meat. *Chemical composition*." 235-243.

Knowlton, J. and Pearce, S. (2013) *Handbook of Cosmetic Science & Technology*. (pp. 389-390). Okford, UK: Elsevier

Koehler, Eric & Amziane, Sofiane & Bui, Van & Deshpande, Yogini & Ferron, Raissa & Hu, Jiong & Li, Zhuguo & Nehdi, Moncef & Pileggi, Rafael & Tanesi, Jussara & Beaupre, Denis & Chidiac, S.E. & Domone, Peter & Fowler, David & Kappi, Aulis & McCarthy, Richard & Ozyildirim, H. & Sobolev, Konstantin & Wang, Kejin & Zhang, Min-Hong. (2014). ACI 238.2T-14 TechNote Concrete Thixotropy. American concrete institute technote. ACI 238.2T-14. Retrieved May 13, 2020, from https://www.researchgate.net/publication/273319359_ACI_2382T-14_TechNote_Concrete_Thixotropy

Koretsky, M. (2013) Engineering and Chemical Thermodynamics (2nd ed.) New Jersey: John Wiley & Sons

LaNasa, P. J., & Upp, E. L. (2014). *Fluid flow measurement: A practical guide to accurate flow measurement*. Amsterdam, Netherlands:Butterworth-Heinemann.

Lawrence, T., & Mancini, R. (2004). Meat: Hot Dogs and Bologna. Smith J.S. and Hui, H.Y. *Food Processing:Principles and Applications*. (pp. 391-397). Iowa: Blackwell Publishing

Li, Q., Gong, J., Zhang, J. 2015. Rheological Properties and Microstructures of Hydroxyethyl Cellulose/Poly(Acrylic Acid) Blend Hydrogels. *Journal of Macromolecular Science Part B: Physics* 54 1132–1143

Li, J. Y., and Yeh, A. I. (2003). Effects of starch properties on rheological characteristics of starch/meat complexes. *Journal of Food Engineering*, *57*(3), 287-294.

Lin, Y (2011). Polymer Viscoelasticity: Basics, Molecular Theories, Experiments, and Simulations. 2nd Edition. Toh Tuck Link, Singapore: World Scientific Publishing Co. Pte. Ltd.

Lonergan, S. M., Topel, D. G., & Marple, D. N. (2018). *Science of Animal Growth and Meat Technology*. Academic Press.

Lotzke, F. and Nyberg, J. (2019). *Compression analysis of primary and secondary package* (Master Thesis, Department of Construction Sciences Solid Mechanics, LTH, Lund University, Lund, Sweden). Retrieved May 3, 2020, from http://lup.lub.lu.se/luur/download?func=downloadFile&recordOId=8947302&fileOId=8947313

Luallen, T. (2018). Utilizing starches in product development. *Starch in food*. (pp. 545-579). Cambridge, UK: Woodhead Publishing.

Mandigo, R. W., and G. A. Sullivan. (2014) Chemistry and Physics of Comminuted Products. *Emulsions and Batters.* (pp. 283-288). NE: Elsevier Ltd.

Marple, D., Lonergan, S., and Topel, D. (2019). Sausage processing and production, Chapter 14. *The Science of Animal Growth and Meat Technology*. (pp. 229-253). London, UK: Academic Press.

Mathisson, J. (2003). Rheology. Bylund, G. *Dairy processing handbook*. (pp. 37-44). Lund, Sweden: Tetra Pak Processing Systems AB

Moisés, G., Alencar, L., Naccache, M., and Frigaard, I. (2018) The influence of thixotropy in start-up flow of yield stress fluids in a pipe. *Journal of Petroleum Science and Engineering*. 171. 794-807

Moller, P., Fall, A., Chikkadi, V., Derks, D., & Bonn, D. (2009). An attempt to categorize yield stress fluid behaviour. *Philosophical Transactions of the Royal Society A: Mathematical, Physical and Engineering Sciences*, *367*(1909), 5139-5155. https://doi.org/10.1098/rsta.2009.0194

Muhammad, A. (2020). Approaches for improving the rheological charcterization of fermented dairy products. Retrieved May 1, 2020, from http://lup.lub.lu.se/luur/download?func=downloadFile&recordOId=9006179&fileOId=9006180

Munson, Bruce R., Young, Donald F., Okiishi, Theodore H., Huebsch, Wade W. (2009). Fundamentals of Fluid Mechanics. (6th ed.). New Jersey: John Wiley & Sons

NPack. (2020). How does a piston filler work? Retrieved May 10, 2020, from https://www.npackfillers.com/piston-filler-work.html

Procarton (2014). Why Choose Cartons? Communication. Retrieved May 10, 2020, from https://www.procarton.com/choose-cartons/communication/

Rapp, B. E. (2016). *Microfluidics: modeling, mechanics and mathematics*. Okford, United Kingdom:William Andrew.

Rajput, R. (2005). *A Textbook of Engineering Thermodynamics*. New Delhi, India: Laxmi Publishing Ltd.

Rao, M (2014) *Rheology of Fluid, Semisolid, and Solid Foods: Principles and Applications* (3rd ed.) New York: Springer

Santhi, D., Kalaikannan, A., & Sureshkumar, S. (2017). Factors influencing meat emulsion properties and product texture: A review. *Critical reviews in food science and nutrition*, *57*(10), 2021-2027. https://doi.org/10.1080/10408398.2013.858027

Şakar-Deliormanli, A (2012) Flow behavior of hydroxypropyl methylcellulose/polyacrylic acid interpolymercomplexes in aqueous media. Polymer International 61 1751-1757

Savarmand, S., Heniche, M., Béchard, V., Bertrand, F., and Carreau, P. (2007). Analysis of the vane rheometer using 3D finite element simulation. *Journal of Rheology*. 51(2). 161-177.

Schwartz, W. C., & Mandigo, R. W. (1976). Effect of salt, sodium tripolyphosphate and storage on restructured pork. *Journal of Food Science*, *41*(6), 1266-1269. https://doi.org/10.1111/j.1365-2621.1976.tb01148.x

Shalaby, A. I. (2018). *Fluid Mechanics for Civil and Environmental Engineers*. CRC Press.

Statista (2020). U.S. population: Consumption of canned meat from 2012 to 2023. Retrieved May 10, 2020, from https://www.statista.com/statistics/320927/us-households-consumption-of-canned-meat-trend/

Steffe, J. (1996) *Rheological Methods in Food Processing Engineering*. (2nd ed.) Michigan: Freeman Press

Smith, D. M. (1988). Factors influencing texture formation in comminuted meats. In *Reciprocal Meat Conference Proceedings*. 41. 48-51

Smith, P (2003) *Introduction to Food Process Engineering*. New York: Plenum Publishers.

Spam. (2019). Spam Varieties. Retrieved May 13 2020 from: https://www.spam.com/varieties/spam-classic

Tetra Pak. (2015a). Tetra Recart. Retrieved May 3, 2020, from https://www.tetrapak.com/packaging/tetra-recart

Tetra Pak. (2015b). Tetra Pak R2. Retrieved May 3, 2020, from https://www.tetrapak.com/packaging/tetra-pak-r2

Tetra Pak. (2020). Tetra Recart. Retrieved May 10, 2020, from https://www.tetrapak.com/packaging/tetra-recart/food-development-centre

Tetra Recart Technical Training. (2014). The Piston filler, Training Document. Lund, Sweden:Tetra Pak

Toledo, R., Cabot, J., and Brown, D. (1977). Relationship between composition, stability and rheological properties of raw comminuted meat batters. *Journal of Food Science*. 42(3) 725-727

Wainwright, E. (2014). [Particle Size Characterization in Turbid Colloidal Suspensions]. Retrieved May 12, 2020, from http://physics.wooster.edu/JrIS/Files/Web_Article_Wainwright.pdf

Wei, Y., Solomon, M., and Larson, R. (2016) Quantitative nonlinear thixotropic model with stretched response in transient shear flows. Journal of Rheology 60 1301-1315

Weiss, J., Gibis, M., Schuh, V., & Salminen, H. (2010). Advances in ingredient and processing systems for meat and meat products. *Meat science*, *86*(1), 196-213. https://doi.org/10.1016/j.meatsci.2010.05.008

Zayas, J. F. (2012). *Functionality of proteins in food*. Heidelberg, Germany: Springer Science & Business Media.

Zhong, Q and Daubert, C. (2013). Food Rheology. Kutz, M *Handbook of Farm, Dairy and Food Machinery Engineering* (2nd ed.). (pp. 403-406). New York: Elsevier Inc.

# Appendix A Work distribution and time plan

## A.1 Work distribution

The Diploma work was performed by two Master students with Food Engineering and Food Technology background. All the activities done which include planning, preliminary experiments, actual experiments in the laboratory and Pilot plant scale, weekly supervision reports, data analysis, and Master thesis writing were equally distributed between the two students.

During the testing in the Pilot plant scale, simultaneous activities like meat production and preliminary water test were equally divided between the two members in order to maximize the time.

The output of each member per activity was discussed and agreement was made each time. This collaboration was needed to achieve the goals of the Master thesis.

## A.2 Project plan and outcome

A timeline was used to guide the planning and schedule of the Diploma work. This included the specific activities to be done the whole master thesis and this was being updated every week to keep track of the progress of the work. The pilot plant testing of the proxy product (model system for meat batter) was replaced by the meat batter testing in the machine due to the unavailability of the raw materials needed to produce large scale of the proxy product. The development of the proxy product was not included in the results and discussion but would be discussed in the Appendix J.

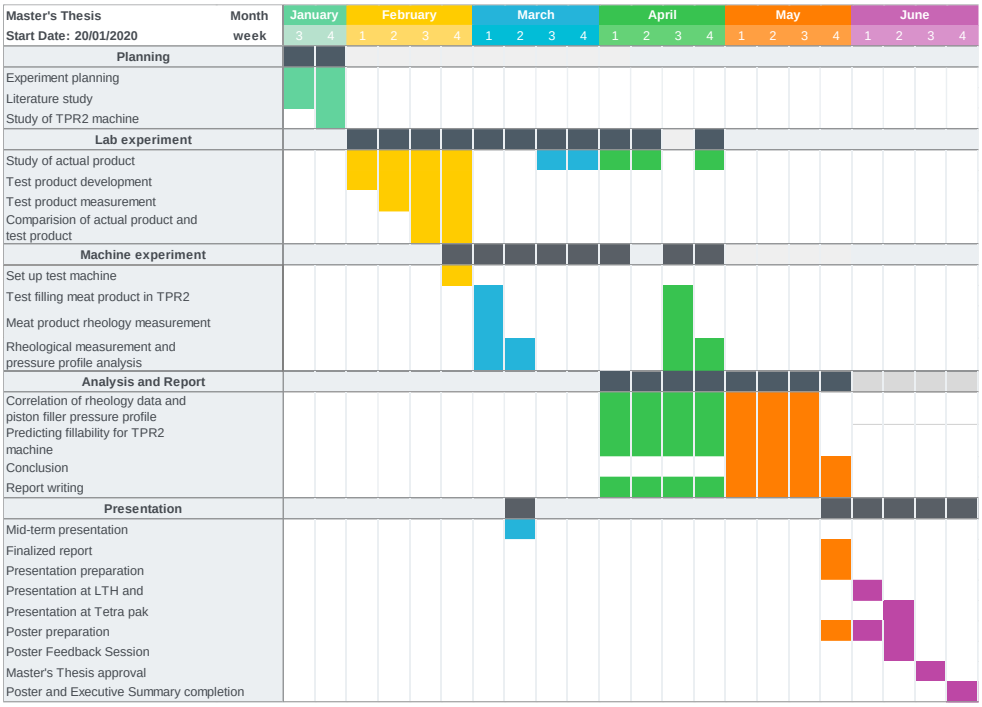


**Figure 45 Time Plan**

# Appendix B Meat Batter Preparation

*This includes the meat batter recipe and the images of the meat during production.*

## B.1 Meat Sample Preparation

### B.1.1 Recipe

There were four different meat samples that were prepared for the analysis with varying amount of added water, pork shoulder, pork belly, and salt tabulated below.

**Table 13 Meat Batter Recipe (Added Water)**

| *Raw Materials* | *10%* | *15%* | *20%* | *30%* |
|---|---|---|---|---|
| Pork belly | 43.5 | 41.04 | 38.6 | 33.7 |
| Pork shoulder | 43.5 | 41.04 | 38.6 | 33.7 |
| Salt | 1.5 | 1.4 | 1.3 | 1.1 |
| Modified starch | 1.5 | 1.5 | 1.5 | 1.5 |
| Water | 10 | 15 | 20 | 30 |
| Total | 100 | 100 | 100 | 100 |

### B.1.2 Raw Materials

The images of the raw materials throughout the whole process can be seen below.

**Figure 46. Before curing (a) pork shoulder and pork belly (laboratory scale) (b and c) pork shoulder and pork belly (pilot plant scale)**

**Figure 47 After curing (a) laboratory scale (b) pilot plant scale**

**Figure 48 After grinding (a) laboratory scale (b) pilot plant scale**

**Figure 49 After mixing (a) laboratory scale (b) pilot plant scale**

# Appendix C Rheometer Procedure

*This includes the detailed procedure for Kinexus Malvern Rheometer.*

1. Turn on the air supply and make sure that the pressure is set at 3-4 bar.
2. Open the rSpace for Kinexus desktop icon to start the software.
3. Remove the Air bearing protection lock.
4. Turn on the machine if the desired pressure is attained.

Stabilization is done by allowing the machine to be turned on for 5minutes before taking measurement.

5. Insert the selected geometery (serrated cup and vane) and lock the geometry release lever.
6. Set the sample loading gap and perform zero gap initialization.
7. Load the sample and make sure that the cup is filled up.
8. Place the sample cover to prevent sample drying and to reduce thermal gradient.
9. Set the temperature for testing.
10. Choose the suitable sequence and modify the following parameters:
    a. Sample per decade- number of samples to be taken per linear or logarithmic decade
    b. Sampling interval-time duration between two sampling points
    c. Shear stress/rate range-initial and final shear stress/rate
11. Start the sequence and wait until the temperature stabilizes. The stabilization can be skipped after one minute once the desired temperature is reached.
12. When the sequence has ended, copy the raw data into Excel file. Make sure that all data needed are selected in the Table properties.
13. Unload the sample in the Software.
14. Unlock the geometry by pulling the cartridge level towards to the left.
15. Clean dry the cup and vane. Return to its original casing.
16. Insert the protective bob and place the sample cover.
17. Close the rSpace software and the computer.
18. Turn off the rheometer.
19. Turn off the air supply.

# Appendix D Preliminary Tests for Rheology: Different Probes

*This includes the preliminary tests for the different probes used for the rheological testing.*

**Table 14 Comparison of different rheology geometry**

| ***Parameter*** | ***Bob and cup*** | ***Smooth bob and cup*** | ***Plate to plate*** | ***Cone and plate*** | ***Vane and serrated cup*** |
|---|---|---|---|---|---|
| Force | The machine needs more force to insert the probe to the sample. Needed force was exceeded 20 N limit. | The machine needs more force to insert to the probe to the sample. Needed force was exceeded 20 N limit. | The geometry contributed to uneven force across plate, thus varied shear over the sample. | N/A | The probe was able to insert to the sample and not exceeded the force limit. |
| Loading sample | Difficulty of loading sample to fill the gap on the side of the cup. | There was some difficulty loading the sample to fill the gap on the side of the cup. | The sample was loaded easily on the plate. | N/A | The loading sample procedure conducted without too much disruption of the sample. |
| Target gap | The rheometer could not reach the target gap due to the product stuck at the bottom of cup. | The rheometer could not reach the target gap due to the product stuck at the bottom of cup. | The rheometer was able to reach the target gap and perform measurement. | N/A | The rheometer able to perform the measurement until the end of sequence. |


**Figure 50 The geometries tested with meat batter sample a) Bob and cup, b) Smooth Bob and cup, c) Plate to plate, d) Cone and plate and e) Vane and serrated cup.**

# Appendix E Pre-shearing Variable

*This presents the preliminary pre-shearing variables conducted.*

**Table 15 Pre-shearing sequences in preliminary test**

| *No.* | *Stabilizing time (s)* | *Pre-shearing ($s^{-1}$)* | *Pre-shearing time (s)* | *Shear rate range ($s^{-1}$)* |
|---|---|---|---|---|
| 1 | 70 | 0 | 0 | 0.1-200 |
| 2 | 70 | 1 | 30 | 0.1-200 |
| 3 | 70 | 10 | 90 | 0.1-200 |
| 4 | 70 | 1 | 120 | 0.1-200 |

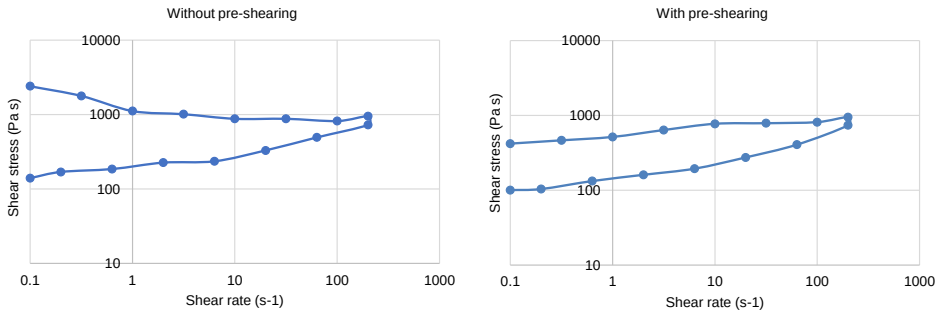


**Figure 51 The flow curve of preliminary test, measurement performed without pre-shearing and with pre-shearing at 10 $s^{-1}$ for 90 s**

Figure 51 shows the comparison between samples without pre-shearing and with pre-shearing. The high shear stress at the beginning of cycle following by dramatic drop were not explainable with rheological equations. However, when pre-shearing was introduced, the flow curve can be fitted with Power Law equation. The application in TPR2 machine also has the agitation in product tank which could be represented by the pre-shearing. After the preliminary test, sequence with pre-shearing at shear rate 10 $s^{-1}$ for 90 s was selected and applied for the sweep up and down rheology measurements with shear rate range from 0.1-200 $s^{-1}$. This is to imitate the agitator and this is sufficient to eliminate the unexplainable phenomena at the beginning but not applying too much shear to the product.

# Appendix F Machine Calibration

*This includes the pressure sensor calibration and water testing data from the Machine testing.*

## F.1 Meat Sample Preparation

The pressure sensors were calibrated by the Tetra Pak Calibration Lab in Lund, and the pressure measurements gathered were corrected using the following factor:

$$Calibrated\ P1 = (P1 * 0.9996) + 0.124 \quad (32)$$

$$Calibrated\ P2 = (P2 * 1.002) + 0.006 \quad (33)$$

## F.2 Meat Sample Preparation

### F.2.1 Methodology

The machine was tested with water with and without agitation at 25Hz. The water was filled into the package at 3000package per hour machine capacity using the same Cam curve profile used for the meat batter. The pressure measurements of P1 and P2 were gathered to compute for the Pressure drop, ΔP (P1-P2).

### F.2.2 Results

Figure 52 shows the pressure measurements for the water flowing through the pipes. It could be observed that as the valve opened, decrease in the pressure measurements followed by a significant increase in the P2 measurement which could mean an occurrence of backflow from the pressure of the piston. During the time when the piston velocity was constant, small oscillations were observed which could mean that the flow may be turbulent. The average experimental ΔP was -20±2.2 hPa. The negative value could mean that there was a back flow during the filling process. Deceleration of the piston resulted to small increase in the P2. As the valve was

closed, significant increase in the pressure measurements were recorded, of which the increase is more dominant with P2. This could mean that there was a backflow caused by the rapid closing of the valve.

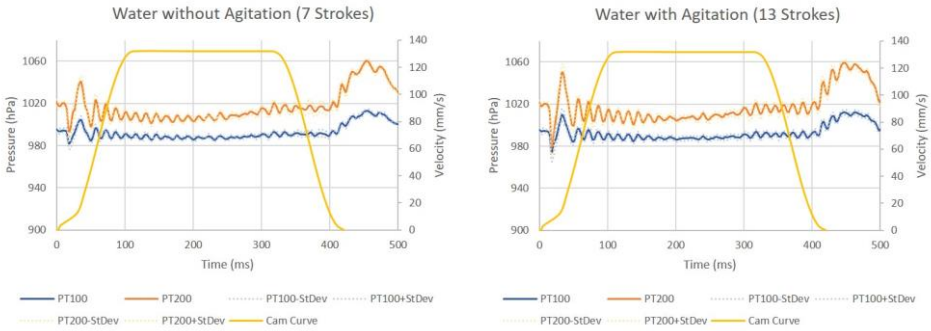


**Figure 52 Pressure Measurements for Water Testing (a) Without Agitation (b) With Agitation**

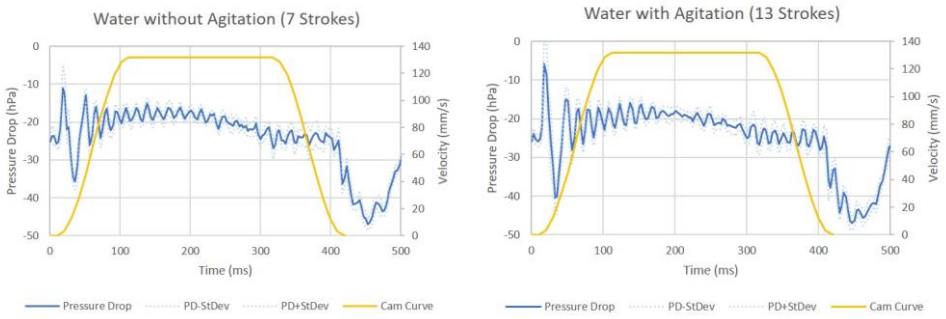


**Figure 53 Pressure Drop for Water Testing (a) Without Agitation (b) With Agitation**

The static pressure of water in TPR2 machine between P1 and P2 was evaluated with Equation (13) and compared with the experimental pressure measurement. The density (ρ) of water is 997 kg/m$^3$, h is 0.175 m and the gravitational acceleration is 9.81 m/s$^2$. Therefore, the static pressure between P1 and P2 is 1711.59 Pa while the pressure measurement is 2600 Pa which gave 34% relative error.

Flow in pipe

From Equation (14), the Reynolds numbers of water at 40°C with $\rho = 992.2\ kg/m^3$, $\nu = 0.132\ m/s$ and $\mu = 0.653 \times 10^{-3}\ \frac{N \cdot s}{m^2}$ flow in pipe with 0.052 m diameter can be calculated as the following

$$Re = \frac{992.2\ \frac{kg}{m^3} \times 0.132\ \frac{m}{s} \times 0.052m}{0.653 \times 10^{-3}\ \frac{N \cdot s}{m^2}} = 10429.5$$

Re > 4000 therefore, the flow is turbulent. Therefore, the $f$ value can be obtained by reading the Moody diagram. According to Gokhale (2011), the absolute pipe roughness ($\varepsilon$) of smooth stainless steel pipe which in this study is 0.015 mm. and the diameter of the pipe is 52 mm. Therefore, the relative pipe roughness ($\frac{\varepsilon}{D}$) is 0.03. Thus, the $f$ for water flow in pipe read from Moody diagram is 0.029 as show in the following Fig. 54.

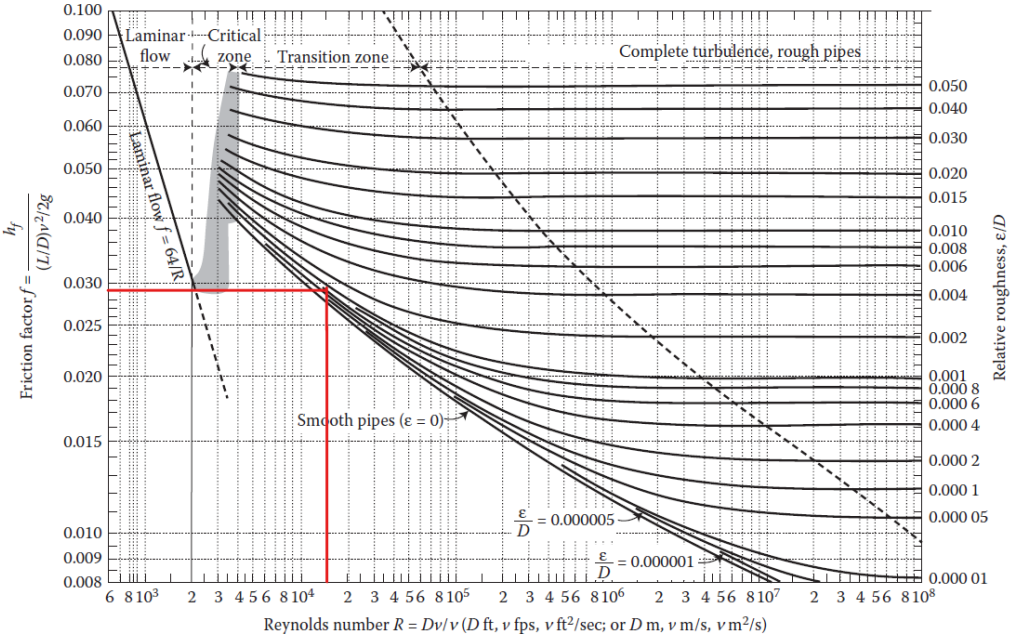


**Figure 54. Moody Diagram**

The pressure drop can be calculated with the Equation (17) as follows:

$$\Delta P = 0.029 \frac{0.175\ m}{0.052\ m} \frac{(0.132 \frac{m}{s})^2}{2} 992.2 \frac{kg}{m^3} = 1.69\ Pa$$

The experimental pressure drop during flow is -20hPa. This could be due to the height elevation of the pipe. And the condition considered by the equation was for flow in the horizontal pipe. The setup of machine also has the piston movement and valve that influenced the flow in section of study.

# Appendix G Breakdown Graphs

*This presents the break down test graphs for 15%, 20%, and 30% AMWB.*

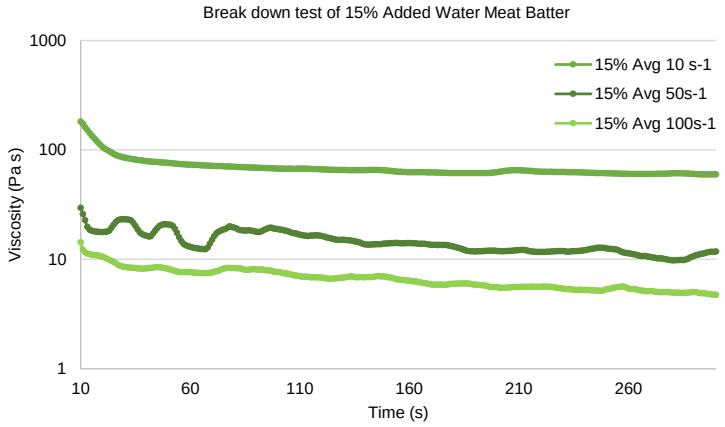


**Figure 55 Break down test for Thixotropic study of laboratory scale 15% AWMB with shear rate 10, 50 and 100 $s^{-1}$**

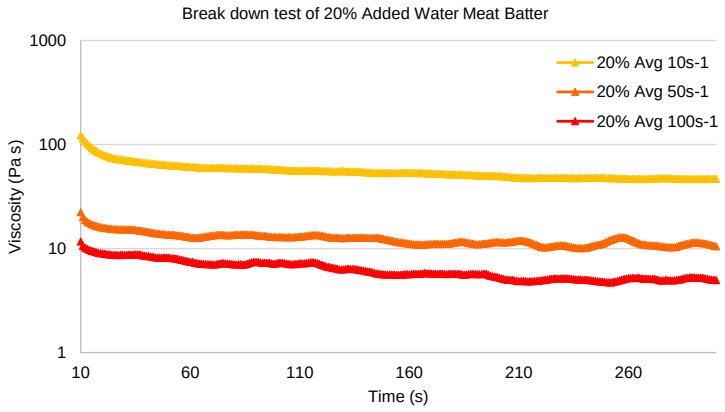


**Figure 56 Break down test for Thixotropic study of laboratory scale 20% AWMB with shear rate 10, 50 and 100 $s^{-1}$**

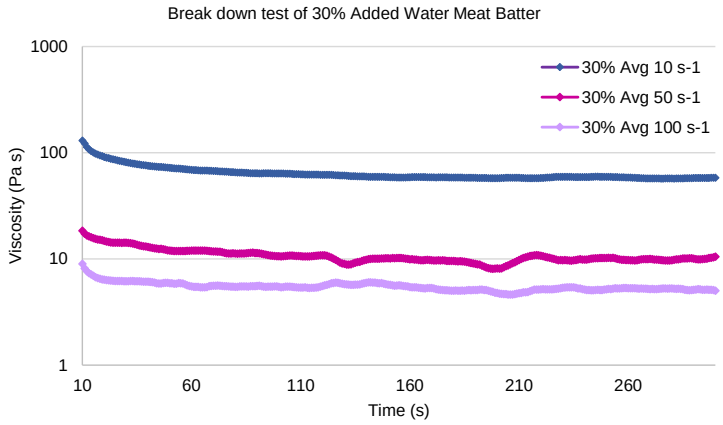


**Figure 57 Break down test for Thixotropic study of laboratory scale 30% AWMB with shear rate 10, 50 and 100 $s^{-1}$**

# Appendix H Build-Up Graphs

*This includes the build-up test graphs for 15%, 20%, and 30% AWMB.*

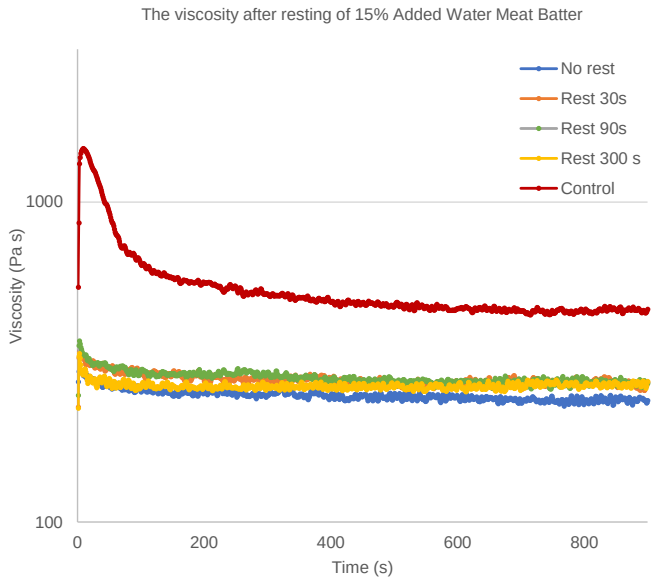


**Figure 58 The build-up test shown the structure recover after resting time (0, 30, 90 and 300 s) of laboratory scale 15% AWMB**

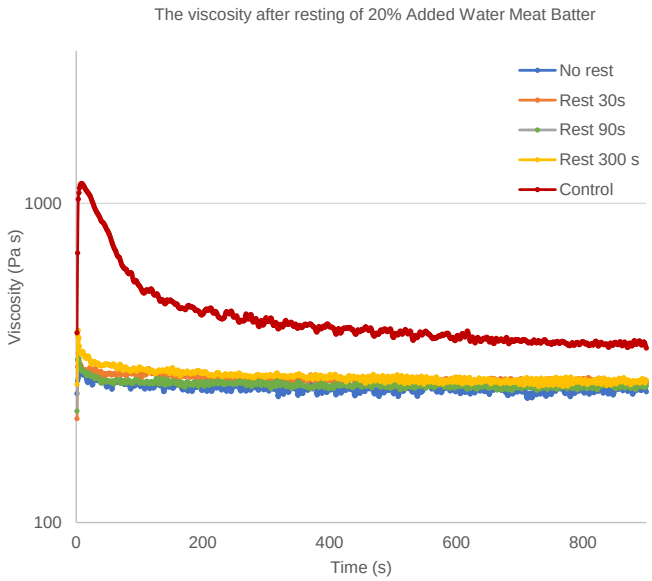


**Figure 59 The build-up test shown the structure recover after resting time (0, 30, 90 and 300 s) of laboratory scale 20% AWMB**

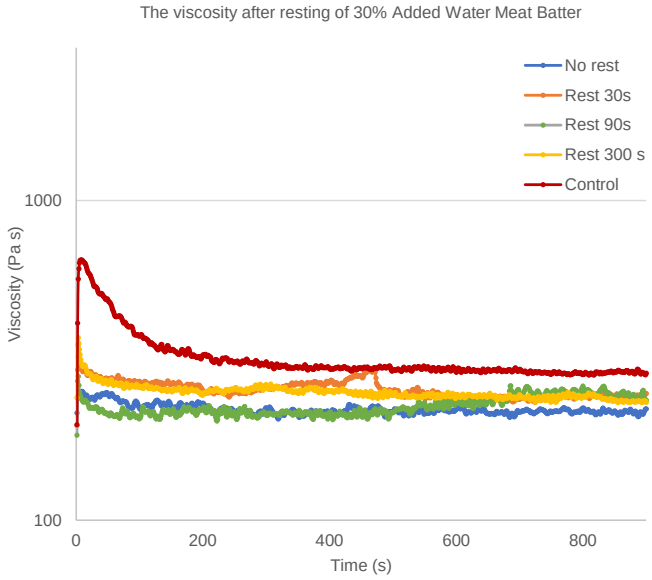


**Figure 60 The build-up test shown the structure recover after resting time (0, 30, 90 and 300 s) of laboratory scale 30% AWMB**

# Appendix I Meat Batter Particle Size

*This details the preliminary test for the meat batter particle size.*

## I.1 Methodology

One gram of the mixture was placed in a 4.5in diameter petri plate with 50mL distilled water (20°C). The meat particles are dispersed in the water and the image was taken to visually compare the particle size and uniformity.

## I.2 Results and Discussion

The meat batter samples were dispersed in deionized water to analyze the particle size. The meat batter samples which were produced during this study showed dissimilar of turbidity between meat batter produced in laboratory scale and pilot plant scale as seen in Figure 61 and 62. As stated in many studies, meat emulsion or meat batter is a very complex matrix. It contains meat protein, meat fibre, fat droplets and other non-meat ingredients. (Hoogenkamp, 2011) Many factors could affect the properties of the meat batter and its stability. (Schwartz and Mandigo, 1976; Santhi, Kalaikannan and Sureshkumar, 2017)

One of the possible reasons for such difference is the method of preparation of the samples. For pilot plant scale, the grinded cured pork was placed into bowl chopper together with starch. The water was gradually added along the mixing process in the bowl chopper thus, the mixing time needed was longer for samples with higher % added water. The end of the mixing process was also dependent with the Tetra Pak Chef. This agrees with some premium meat emulsion production line in which the time and speed of chopping were adjusted by expertise to obtain the finest properties of the product. (Hoogenkamp, 2011) Meanwhile in laboratory scale procedure, the water was added at the same time with other ingredients and was mixed in smaller food processor with fixed duration. Across the four samples, the lean meat particles were hardly distinguished from fat particle.

On the other hand, the difference between the meat batter produced at Laboratory scale and Pilot plant scale was obviously identified due to the level of turbidity of continuous phase. This could be explained by the light scattering phenomena as more small meat particles are distributed in the continuous phase. The phenomena related to intensity of the light transmission and the light incident. (Wainwright, 2014)

Bowl chopper is commonly used for mixing small to very small lean meat and fat particles with other ingredients. (Weiss, Gibis, Schuh and Salminen, 2010) The set of rotation curve knives manipulate the flow of the meat batter in revolving bowl which results to homogeneous matrix. Household food processor, on the other hand, contains two horizontal rotational blades. This could generate more heat to the mixture that would affect the meat batter properties. Also, overdoing particle reduction could result in decrease of emulsification. (Devatkal, et al., 2014; Schwartz and Mandigo, 1976)

Kang, Li, Ma and Chen (2016) study showed that the different equipment being used in meat batter production significantly influenced the properties of meat batter. Gorbatov and Gorbatov (1970) as cited in Gorbatov and Gorbatov (1972) believed that this is influenced by the different geometric dimensions and kinematics of the equipment. It also stated by Devatkal, et al. (2014) that the result of using different equipment for particle size reduction on meat batter were hardly identified. In their study, the meat batter prepared with bowl chopper was the most effective meat comminutor as result of high product yield with more stable meat batter compared to food processor.

Nevertheless, there were limited literature investigated on the particle size and turbidity of meat batter. The turbidity measurement need to be conducted to qualified the level of turbidity and differences between laboratory and pilot scale samples in this aspect.

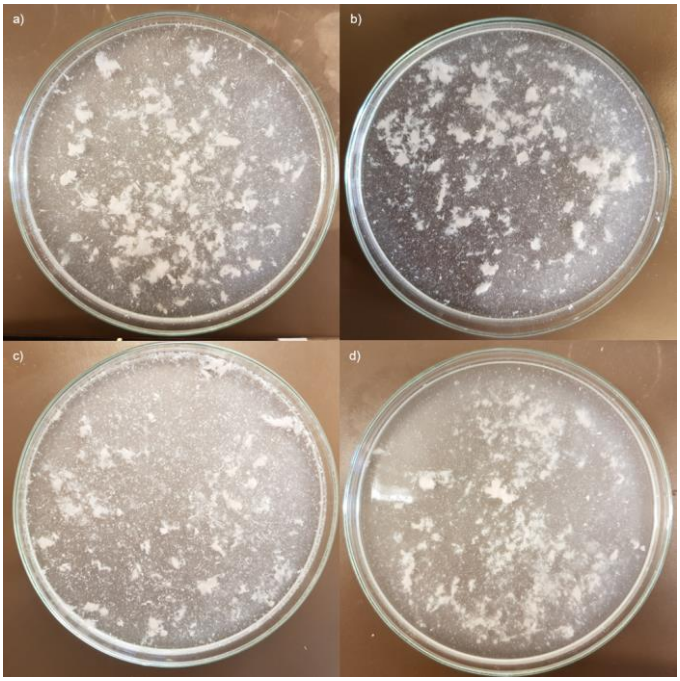


**Figure 61 The particle investigation of laboratory scale meat batter a) 10% AWMB, b) 15% AWMB, c) 20% AWMB and d) 30% AWMB**

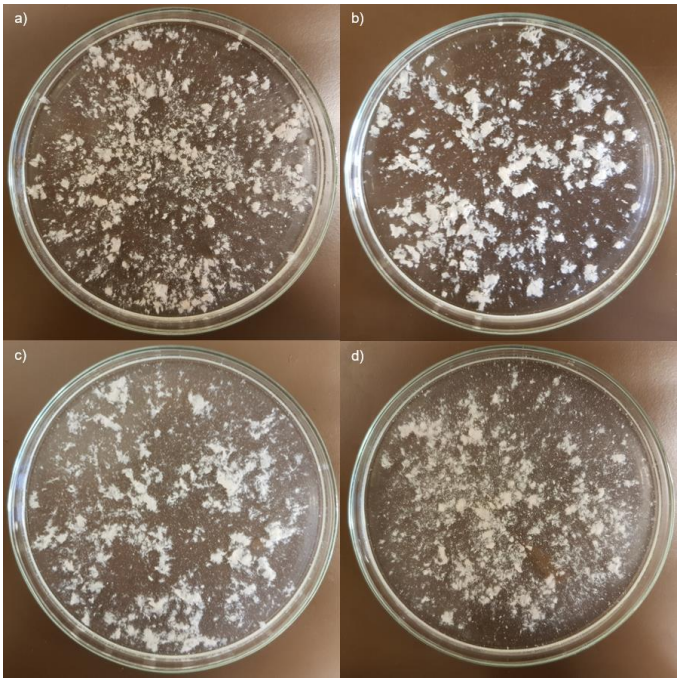


**Figure 62 The particle investigation of pilot scale meat batter a) 10% AWMB, b) 15% AWMB, c) 20% AWMB and d) 30% AWMB**

# Appendix J Proxy Products

*This contains the initial experiments on the development for proxy or substitute products.*

## J.1 Materials

Carbopol 974P NF (BF Goodrich) and medium Cellulose fibers (Sigma Life Science) were purchased. Distilled water was used for the whole experiment.

## J.2 Methodology

The base of the proxy product was prepared by slowly adding specific weight of Carbopol (5g for 1% and 15g for 3%) to 500g distilled water (20°C) using Omni-mixer Sorvall at setting 1.5. The mixture was then mixed for 5mins at incremental speed until setting no. 7. The carbopol hydrogel was then neutralized by slowly adding 0.1N NaOH and mixing the gel to attain the desired pH of 5, 6, 7, and 9. Medium cellulose fiber was added at 30% (w/w) by adding 30g cellulose to 70g of hydrogel. The sample was manually mixed until the cellulose has been dispersed properly.

### J.2.1 Rheometer Testing

The same protocol for the meat samples was implemented. The samples were measured for sweep up and down using the same sequence to compute for the rheological parameters. The data gathered were also analyzed for linear and logarithmic method using OLS.

### J.2.2 Rheogram Presentation

The shear stress was plotted against the shear rate and the Power Law model was used to compute for the rheological parameters, K and n value using the OLS method. The apparent viscosity was computed using these values.

## J.3 Results and Discussion

Figures 63-68 on the left show the different proxy products made up of Carbopol with different concentration (1% and 3%) and pH (5, 6.3, 7, and 9). It could be observed that hydrogels made of Carbopol followed the non-Newtonian behavior in which the shear stress changed as the shear rate changed. Also, the rheograms or flow curve showed that Carbopol solutions do not exhibit strong thixotropy property. 1%

Blends of Carbopol suspension with Cellulose (medium fiber) were made to improve the thixotropic property of the proxy product. Figures 63-68 on the right showed the flow curves for these blends. Addition of the cellulose shifted the flow curve to higher shear stress for all the mixtures. It was also observed that the area in between the sweep up and down of the flow curve for the blend were larger compared to the pure Carbopol suspensions. Li, Gong, Zhang (2015) studied the combination of Hydroxyethyl Cellulose/Poly(Acrylic Acid) which results to the formation of interpenetrating network (IPN). They observed that the blend followed the Ostwald-de Waele power law model. The increase in the shear rate applied increased the shear stress greater than the interactions such as hydrogen bonding, Van der Waals forces, and ionic interactions which resulted to the flow. (Watanabe, Morita, and Ozaki, 2006 as cited by Li et al, 2015)

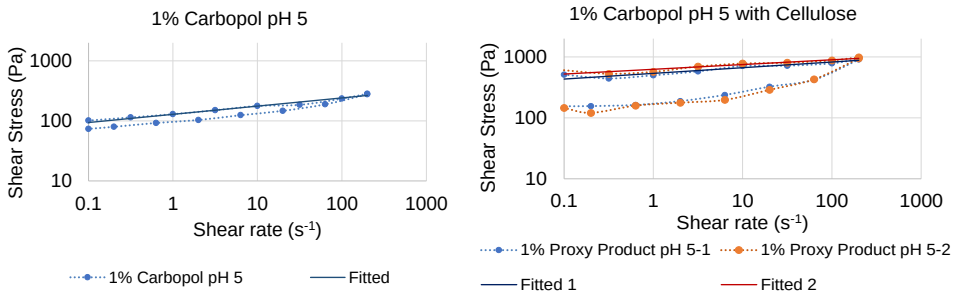


**Figure 63 1% Proxy Product pH 5 (a) 1%Carbopol (b) 1% Carbopol with Cellulose**

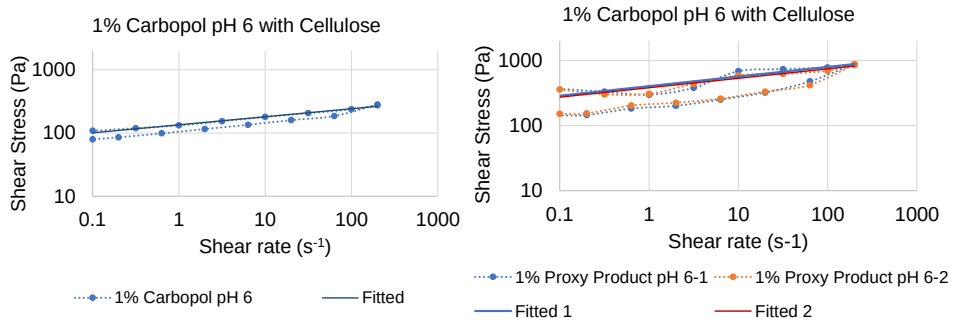


**Figure 64 1% Proxy Product pH 6 (a) 1% Carbopol (b) 1% Carbopol with Cellulose**

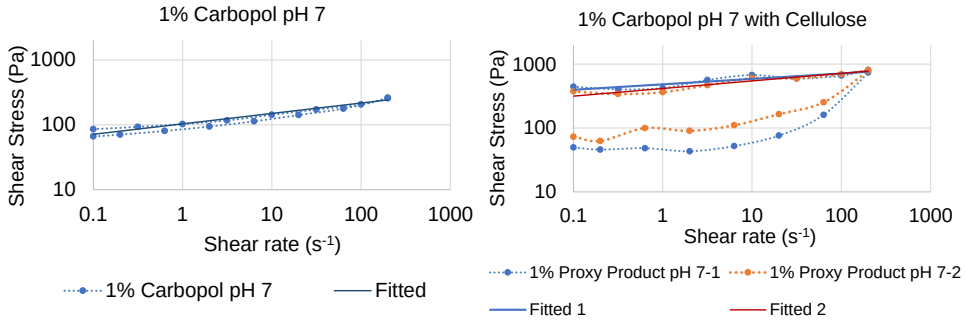


**Figure 65 1% Proxy Product pH 7 (a) 1% Carbopol (b) 1% Carbopol with Cellulose**

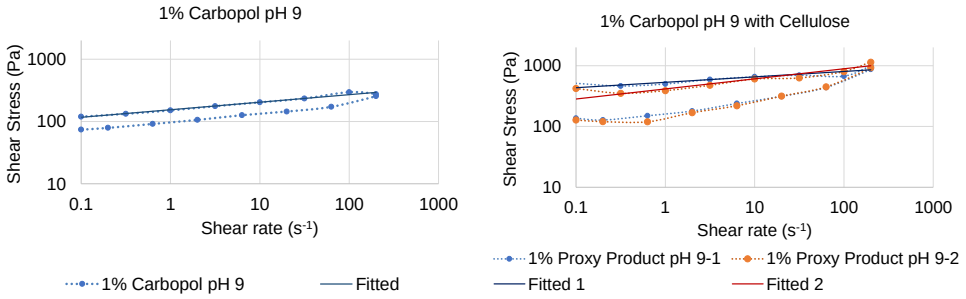


**Figure 66 1% Proxy Product pH 9 (a) 1% Carbopol (b) 1% Carbopol with Cellulose**

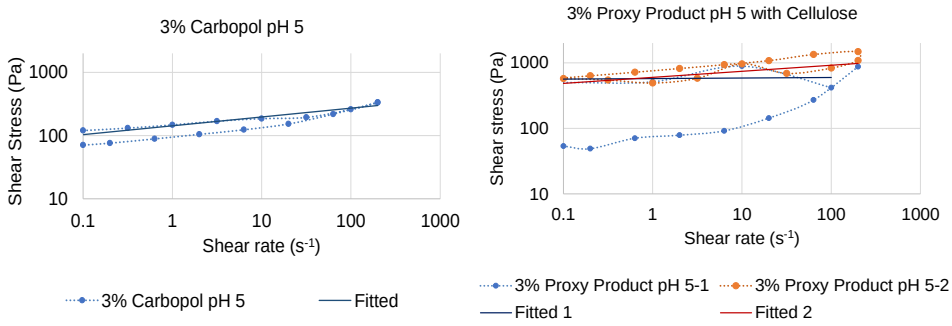


**Figure 67 3% Proxy Product pH 5 (a) 1% Carbopol (b) 1% Carbopol with Cellulose**

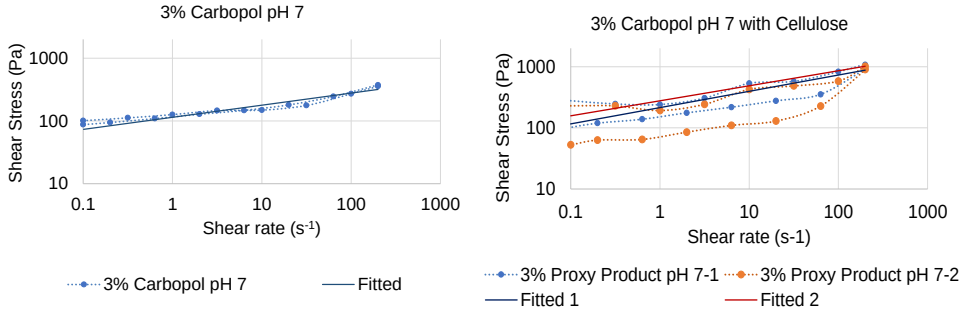


**Figure 68 3% Proxy Product pH 7 (a) 1% Carbopol (b) 1% Carbopol with Cellulose**

Table 16 shows the rheological parameters for different proxy products. It was evident that the K values for Carbopol were significantly lower than those of Carbopol/Cellulose blend. It could be seen that the 3% pH 5 Carbopol/Cellulose blend had the largest K value among the mixtures. There was a decreasing trend from pH 6 to pH 7 and increasing trend of K value as the pH was increased from pH 6 until pH 7 for 1% Carbopol. The same decreasing trend was seen with the 3% Carbopol hydrogels from pH 5 to pH 7.

The n values did not show any trend as compared across different Carbopol concentration and pH.

**Table 16 Rheological Parameters of Proxy Product**

| | | *K value* | | *n value* | |
|---|---|---|---|---|---|
| ***Carbopol concentration (w/v)*** | pH | Carbopol | Carbopol/ Cellulose Blend | Carbopol | Carbopol/ Cellulose Blend |
| 1% | 5 | 128 | 582±63 | 0.14 | 0.09±0.01 |
| | 6 | 135 | 393±15 | 0.13 | 0.15±0.002 |
| | 7 | 103 | 449±49 | 0.16 | 0.10±0.02 |
| | 9 | 155 | 474±84 | 0.12 | 0.13±0.05 |
| 3% | 5 | 143 | 588±18 | 0.14 | 0.05±0.06 |
| | 7 | 114 | 246±45 | 0.19 | 0.26±0.01 |

The calculated apparent viscosity values at shear rate $32s^{-1}$ were tabulated below. The apparent viscosity for Carbopol for all pH and concentrations were lower than Carbopol/Cellulose blend. The proxy products have similar apparent viscosity with that of 15% AWMB. The values are higher than 20% and 30% but lower than 10% AWMB.

**Table 17 Apparent Viscosity (Pa-s) of Proxy Products**

| | | *Apparent viscosity (Pa-s)* | |
|---|---|---|---|
| ***Carbopol concentration (w/v)*** | pH | Carbopol | Carbopol/Cellulose Blend |
| 1% | 5 | 6.5 | 25±1.3 |
| | 6 | 6.6 | 21±0.7 |
| | 7 | 5.7 | 20±0.4 |
| | 9 | 7.4 | 23±0.2 |
| 3% | 5 | 7.3 | 22±3.7 |
| | 7 | 7.1 | 19±1.7 |

Şakar-Deliormanli (2012) studied the flow behavior of hydroxypropyl methylcellulose/polyacrylic acid interpolymercomplexes which showed that the increase in the viscosity at more basic pH was due to “high ionization degree and coil to stretch structure transition of Polyacrylic acid”. However further increase in the pH results to inorganic salts that weakens cellulose-PAA interaction and increasing the intermolecular in PAA.